PB86-164910

Analytical Parameterizations of Diffusion The Convective Boundary Layer

(U.S.) Environmental Protection Agency
Research Triangle Park, NC

1985

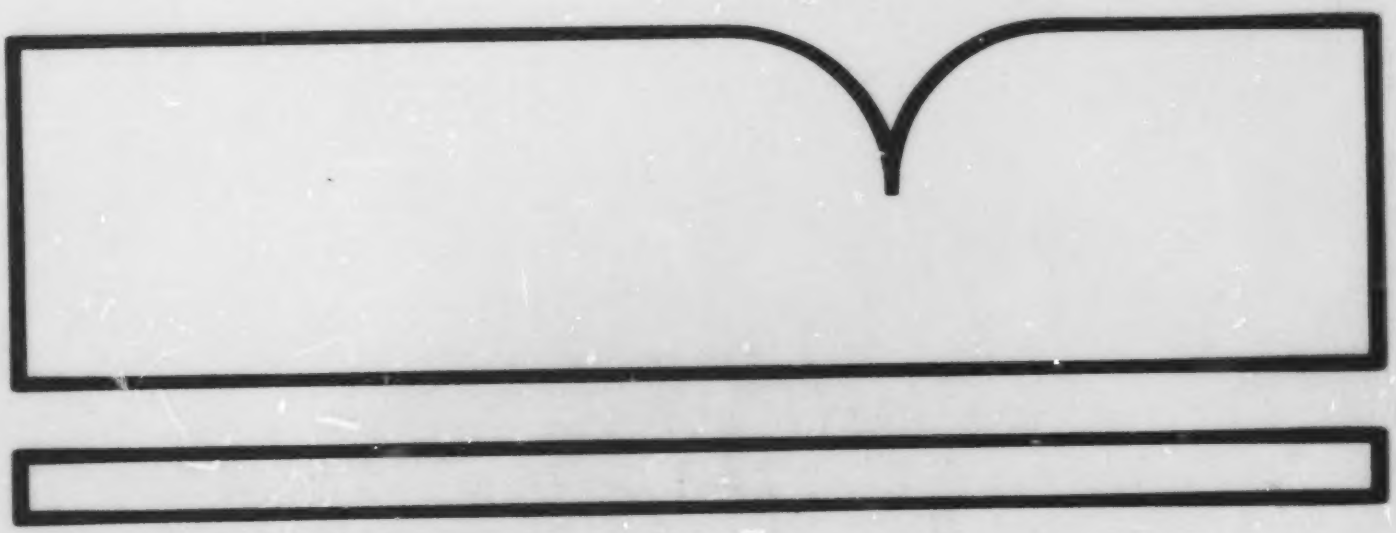

U.S. Department of Commerce
National Technical Information Service
NTIS

TECHNICAL REPORT DATA
(Please read Instructions on the reverse before completing)

1. REPORT NO. EPA/600/J-85/314	2.	3. RI PB86-164910
4. TITLE AND SUBTITLE Analytical Parameterizations of Diffusion: The Convective Boundary Layer (Journal Version)		5. REPORT DATE 1985 6. PERFORMING ORGANIZATION CODE
7. AUTHOR(S) Gary A. Briggs		8. PERFORMING ORGANIZATION REPORT NO.
9. PERFORMING ORGANIZATION NAME AND ADDRESS Meteorology and Assessment Division Atmospheric Sciences Research Laboratory U.S. Environmental Protection Agency Research Triangle Park, NC 27711		10. PROGRAM ELEMENT NO. CDTA1D/03-1361 (FY-85) 11. CONTRACT/GRANT NO.
12. SPONSORING AGENCY NAME AND ADDRESS Atmospheric Sciences Research Laboratory--RTP, NC Office of Research and Development U.S. Environmental Protection Agency Research Triangle Park, NC 27711		13. TYPE OF REPORT AND PERIOD COVERED 14. SPONSORING AGENCY CODE EPA/600/09

15. SUPPLEMENTARY NOTES
REF: J. Climate and Appl. Meteorol., 24(11):1167-1186, Nov. 1985

16. ABSTRACT

A brief review is made of data bases which have been used for developing diffusion parameterizations for the convective boundary layer (CBL). A variety of parameterizations for lateral and vertical dispersion, σ_y and σ_z, are surveyed; some of these include mechanical turbulence, source height, or buoyancy effects. Recommendations are made for choosing among these alternatives, depending on the type of source. Because observations of passive plumes indicate that the Gaussian model does a poor job of describing vertical diffusion in the CBL, alternative models for predicting dimensionless crosswind integrated ground concentration, C_y, are reviewed and compared. These include an analytical equation which closely approximates laboratory results; this equation can be applied to any source height > $0.04z_i$, where z_i is the mixing depth. An analysis of a limited amount of buoyant plume data indicates that a radically different approach is needed when the dimensionless buoyancy flux, F^*, exceeds 0.1. Such plumes impinge on the "lid" of the mixing layer before ground impact occurs, and residual plume buoyancy causes enhanced lateral spreading under the lid; the observations indicate that σ_y approximates the $x^{2/3}$ law that applies to buoyant plume rise when $F^* > 0.06$. The residual buoyancy also causes a delay in downward mixing that is proportional to F^*. The main consequence of these two effects is that maximum ground concentration is reduced, compared to that from passive plumes, and is independent of wind speed. For smaller F^*, the observations indicate that, with an assumed plume rise $\Delta h = 3z_i F^{*3/5}$, several different C_y parameterizations give satisfactory results, including a Gaussian model.

17. KEY WORDS AND DOCUMENT ANALYSIS

a. DESCRIPTORS	b. IDENTIFIERS/OPEN ENDED TERMS	c. COSATI Field/Group

REPRODUCED BY
NATIONAL TECHNICAL
INFORMATION SERVICE
U.S. DEPARTMENT OF COMMERCE
SPRINGFIELD, VA. 22161

18. DISTRIBUTION STATEMENT RELEASE TO PUBLIC	19. SECURITY CLASS (This Report) UNCLASSIFIED	21. NO. OF PAGES 22
	20. SECURITY CLASS (This page) UNCLASSIFIED	22. PRICE

EPA Form 2220-1 (9-73)

NOTICE

This document has been reviewed in accordance with U.S. Environmental Protection Agency policy and approved for publication. Mention of trade names or commercial products does not constitute endorsement or recommendation for use.

This article documents research that was conducted under the auspices of the U.S. Environmental Protection Agency (USEPA). As an arm of the government, the USEPA has a paid up, non-exclusive, irrevocable, worldwide license to reproduce, prepare derivative works, and distribute to the public all of the material contained herein, and to grant others acting on its behalf the right to do so. The USEPA grants to the National Technical Information Service, Department of Commerce, the right to act as its agent in the distribution of this material.

EPA/600/J-85/314
JOURNAL ARTICLE

Reprinted from JOURNAL OF CLIMATE AND APPLIED METEOROLOGY, Vol. 24, No. 11, November 1985
American Meteorological Society
pp 1167-1186

Analytical Parameterizations of Diffusion: The Convective Boundary Layer

GARY A. BRIGGS*

Meteorology and Assessment Division, Atmospheric Sciences Research Laboratory/EPA, Research Triangle Park, NC 27711

(Manuscript received 17 January 1985, in final form 19 April 1985)

ABSTRACT

A brief review is made of data bases which have been used for developing diffusion parameterizations for the convective boundary layer (CBL). A variety of parameterizations for lateral and vertical dispersion, σ_y and σ_z, are surveyed; some of these include mechanical turbulence, source height, or buoyancy effects. Recommendations are made for choosing among these alternatives, depending on the type of source. Because observations of passive plumes indicate that the Gaussian model does a poor job of describing vertical diffusion in the CBL, alternative models for predicting dimensionless crosswind integrated ground concentration, C_y, are reviewed and compared. These include an analytical equation which closely approximates laboratory results; this equation can be applied to any source height $> 0.04z_i$, where z_i is the mixing depth. An analysis of a limited amount of buoyant plume data indicates that a radically different approach is needed when the dimensionless buoyancy flux, F^*, exceeds 0.1. Such plumes impinge on the "lid" of the mixing layer before ground impact occurs, and residual plume buoyancy causes enhanced lateral spreading under the lid; the observations indicate that σ_y approximates the $x^{2/3}$ law that applies to buoyant plume rise when $F^* > 0.06$. The residual buoyancy also causes a delay in downward mixing that is proportional to F^*. The main consequence of these two effects is that maximum ground concentration is reduced, compared to that from passive plumes, and is independent of wind speed. For smaller F^*, the observations indicate that, with an assumed plume rise $\Delta h = 3z_iF^{*3/5}$, several different C_y parameterizations give satisfactory results, including a Gaussian model.

1. Convective scaling and CBL diffusion

Since 1970, there has been great progress in our knowledge of turbulence structure and flux profiles of the daytime, convective boundary layer (CBL). Some of this improved knowledge has been applied to design of new diffusion experiments, new diffusion models based on more complete physics, and new diffusion parameterizations using more effective physical parameters.[1] The basis for much of this progress is convective scaling, which has proven to be an effective and concise means for describing the more salient features of boundary layer turbulence and diffusion in convective conditions, that is, during daytime, when there is no heavy cloud cover or brisk wind.

Convective scaling, as applied to the atmosphere, was first suggested by Deardorff (1970a,b), who discovered that it conveniently ordered velocity and temperature variances produced in the most convection-dominated runs of his numerical boundary-layer model; furthermore, when the variances were nondimensionalized with convective scaling parameters, they agreed well with aircraft turbulence measurements by Lenschow (1970). Much of the history of the development and testing of convective scaling is given in a recent review (Briggs, 1985), and will not be detailed here.

Like surface-layer similarity scaling, the convective scaling method uses the surface sensible heat flux, or more properly, the density fluctuation flux, as one principal parameter. A convenient form for this is $H^* = (g/\overline{T_v})\overline{w'T_v'}$ (g is gravitational acceleration, T_v absolute virtual temperature, w vertical velocity, a bar denotes a time-averaged value). However, convective scaling uses the depth of convective mixing, z_i, as the principal length parameter, in place of the Obukhov length, $L = -u^{*3}/kH^*$ (u^* is the friction velocity and k is the von Karman constant). This acknowledges the important role of the largest turbulent eddies, which extend vertically through the entire boundary layer in convective conditions, and are more or less isotropic. It follows that the principal scale for turbulence velocities is $w^* = (H^*z_i)^{1/3}$, in place of u^*, used in surface-layer similarity scaling, and the scale for temperature fluctuations is $\theta^* = \overline{w'T'}/w^*$, in place of $T^* = \overline{w'T'}/(ku^*)$ (T is absolute temperature). (See Briggs, 1985, for a derivation of w^* and θ^* based on a simple energy balance argument.) Some typical values for a convective situation in our atmosphere are $z_i = 1000$ m, $H^* = 0.008$ m^2 s^{-3}, $w^* = 2$ m s^{-1}, and $\theta^* = 0.1$°C.

Convective scaling was first applied to diffusion observations by Deardorff and Willis (1975), who also

* On assignment from the National Oceanic and Atmospheric Administration, U.S. Dept. of Commerce.

[1] In this paper, "parameterization" and "analytical equation" refer to an algebraic combination of parameters, i.e., models that do not require solution of differential equations.

made the first suggestions for parameterizations of diffusion coefficients based on this scaling. Their observations were all made in the laboratory, and basically consisted of inventories of the positions of thousands of oil droplets released into convective turbulence produced in a 1.1 m-square water tank with a heated bottom. They convective scaled the results by defining H^* in terms of flux of density fluctuations produced by the surface heat flux, and by using the coefficient of thermal expansion of water in place of $1/T_v$ for an ideal gas. This enabled comparisons with atmospheric diffusion. By using x/U in place of time after release (the tank experiments employed an instantaneous line source), assuming z_i values between 1 and 2 km, and using wind direction variances associated with each dispersion curve in conjunction with $\sigma_a \approx \sigma_v/U \propto w^*/U$, Willis and Deardorff (1976a) were able to show rough agreement between the results of their first series of tank experiments and the Brookhaven and the Pasquill–Gifford dispersion curves (Singer and Smith, 1966; Pasquill, 1961; Gifford, 1961) (x is distance downwind of a continuous point source, U is the mean wind speed in the mixing layer; σ_a is the variance of lateral wind direction, and σ_v is the variance of lateral wind speed).

The most unexpected plume behavior that Willis and Deardorff observed with their near-surface releases was a lifting of the mode of maximum concentration at $t \geq 0.5z_i/w^*$; this accompanied a rapid decrease in surface concentrations. In retrospect, it seems likely that this behavior is caused by convergence of flow near the surface into the bases of updrafts, and the replacement of the near-surface fluid with "clean" fluid (water or air) from downdrafts (see Willis and Deardorff, 1976b). This plume behavior provides an explanation of the Pasquill (1961) "A" and "B" curves for the vertical dispersion coefficient, σ_z, which grow very rapidly with x at distances beyond a few hundred meters. These curves are based primarily on the Prairie Grass experiment (Barad, 1958), which beyond 100 m consisted of only surface measurements of SO_2 concentrations from a source near the ground. Because the σ_z analysis assumed a half-Gaussian plume with its maximum at the surface, so that σ_z would be proportional to $(\int \chi_0 dy)^{-1}$, the rapid decrease in surface concentrations with x was interpreted as a rapid increase in σ_z ($\int \chi_0 dy$ is the crosswind-integrated surface concentration). However, the half-Gaussian vertical distribution assumption leads to overestimation of σ_z if the concentration maximum actually lifts off the surface, as observed in the tank experiments.

2. Diverse and incomplete experimental verification

The first reinforcement of Willis and Deardorff's (1976a) laboratory observations was in the form of numerical experiments by Lamb (1979). He used the computed velocity and turbulence fields from the large-eddy simulation model of Deardorff (1972), tracing the motions of thousands of particles "released" into this numerical flow field. He did this for source heights, z_s, corresponding to $z_s/z_i = 0.026$, 0.26, 0.52, and 0.74, and nondimensionalized the results using convective scaling. The results for $z_s/z_i = 0.026$ were similar to those from the tank experiments, which were run with $z_s/z_i = 0.067$, except that the concentrations at distances greater than $0.5U(z_i/w^*)$ did not reduce quite as rapidly or as much as they did in the tank (using t in place of x/U).

For the more elevated releases, Lamb (1979) found that the mode of maximum concentration descended from the source height to near the surface. The descent rate was approximately $0.5w^*$. The resulting surface concentrations were higher by as much as a factor of 3 than values given by Gaussian plume modeling (with the maximum remaining at source height); this effect increases with increasing z_s/z_i. Farther downwind, the concentration maximums lifted to loft in the upper part of the mixed layer, just as occurred with the near-surface releases. The results of these experiments provided incentive for further tank experiments (Willis and Deardorff, 1978, 1981). These were done for $z_s/z_i = 0.24$ and 0.49, and confirmed the basic patterns of the numerical modeling results. Lamb (1978) pointed out that the convective eddies produced in the numerical model are long-lived, and that downdrafts occupy a greater fraction of the horizontal area than do updrafts. Hence the majority of material from elevated sources is released into downdrafts, which accounts for the descending maximum concentration.

Naturally, the numerical model and tank experiment results provoked interest in testing atmospheric dispersion data in terms of convective scaling. However, the most necessary parameter for this is z_i, the mixing depth, which until 1973 was rarely measured during meteorological field experiments. Among historic diffusion experiments, only the Prairie Grass program included vertical soundings that allow z_i to be determined for most runs. Briggs and McDonald (1978) did this, and estimated H^* from wind and temperature profiles on the 16-m tower and established flux-profile relationships. They showed that the crosswind-integrated concentrations on the Prairie Grass surface arcs agreed with the surface concentrations measured in the tank experiment, when both were nondimensionalized according to convective scaling [$z_i U \int \chi_0 dy/Q = C_y$ versus $X = (x/U)w^*/z_i$ or $T = tw^*/z_i$, where Q is source strength]. Nieuwstadt (1980) also used these data, showing that over most of their range in X they fit the free convection asymptote $\int \chi_0 dy/Q \propto (U/H^*)^{1/2}x^{-3/2}$ (in a free convection layer, z is the dominant scale, rather than L or z_i; the free convection asymptote can be written in convective scaling as $C_y \propto X^{-3/2}$; z_i cancels out of this expression). He also showed that the Prairie Grass σ_y values parallel those of the tank experiments when convectively scaled; the field values average a

factor of 1.4 larger, which Nieuwstadt attributed in part to the confining effect of the tank walls, which were at a distance $\pm 2z_i$ from the line source.

While the agreement among Prairie Grass field data, laboratory tank observations, and numerical model predictions is reassuring, this field experiment was rather limited. Only surface releases were made, and the concentration measurements were made only at $z = 1.5$ m, except for towers on the 100-m arc. The arcs extended only to $x = 0.8$ km, and the duration of the releases was only 10 min; this is insufficient for good ensemble averaging, since individual convective eddies have a passage time of the order of $1.5z_i/U$, which ranged from about 1 to 9 min. Meteorologically adequate field diffusion experiments are needed for larger distances, longer release times, and elevated releases.

Results from two European experiments with elevated SF_6 releases and concurrent mixing depth measurements have recently become available. The runs at Cabauw in the Netherlands (Agterberg *et al.*, 1983) were predominantly neutral, but five 30-min runs can be considered slightly convective (Briggs, 1985). The release height for these runs was 200 m. Surface concentrations were measured on a single measuring arc, at a distance from the source averaging 3.7 km. Similar releases were made at a height of 115 m on a TV tower in the northern suburbs of Copenhagen, with samplers on arcs at $x \approx 2$, 4, and 5.5 km (Gryning, 1981). Six of the ten 1-h sampling periods were considered somewhat convective. More recently, simultaneous surface and elevated releases at $z \approx 250$ m were made at the Boulder Atmospheric Observatory (BAO) in Colorado. Passive tracers were sampled on a single arc at $x \approx 1.2$ km, and oil fog and metalized chaff plumes were scanned in three dimensions using a lidar and a 3-cm radar, respectively. Two-hour releases were made on 12 days in conditions that ranged from moderately to very convective. Processing and analysis of the BAO data are incomplete at present, but some preliminary results have been reported by Moninger *et al.* (1983) and Briggs (1985). These results and those of the five Cabauw runs give reasonably good agreement with the results of Willis and Deardorff's tank experiments, when all are convectively scaled, except that two averaging periods at the BAO had about double the σ_y/z_i values at several kilometers downwind (σ_y is the lateral dispersion coefficient). This was likely due to the large wind direction shear present on that particular day (Briggs, 1985). On the other hand, the nondimensionalized $\int \chi_0 dy$ values reported by Gryning exceed the Willis and Deardorff values at any given X by factors ranging from about 1.4 to 2, for $Z_s = z_s/z_i$ ranging from 0.06 to 0.1 (the one other period, with $Z_s = 0.14$, gives much better agreement). Since C_y drops rapidly with increasing X in these measurements, another interpretation is that the Copenhagen C_y values dropped off more slowly with w^*t/z_i than those in the tank, by roughly a factor of 1.7. In both the Cabauw and the Copenhagen experiments, the arcs appear to have been beyond the distance of maximum C_y.

Some observations of σ_y and σ_z for elevated, buoyant sources have been compared favorably with the laboratory results of Willis and Deardorff (1976a, 1978, 1981), and the numerical results of Lamb (1979); however, because of buoyancy effects, these comparisons always involve additional assumptions. These attempts to apply convective scaling results to models for very buoyant plumes will be discussed in the next sections, since they incorporate suggested parameterizations for diffusion in the CBL.

3. Parameterizations for σ_y

There are basically two different methods used for parameterizing vertical diffusion: one is conventional Gaussian modeling using an analytical equation for σ_z (see section 4), and the other directly parameterizes the crosswind-integrated surface concentration (see section 5). The latter method is capable of accommodating non-Gaussian vertical diffusion effects. However, significantly and systematically non-Gaussian plume shapes have not been observed in the case of lateral diffusion; therefore all analytical models have retained the usual Gaussian form, $\chi \propto \exp\{-[(y/\sigma_y)^2/2]\}$. Any of the parameterizations for σ_y given in this section could be used, depending on modeling needs, source type, dominant meteorology, etc.; thus, I have chosen to evaluate them independently of the "model package" in which they were originally placed.

The first parameterization for the lateral dispersion coefficient, σ_y, in terms of convective scaling was suggested by Deardorff and Willis (1975):

$$\sigma_y/z_i = 0.51X/(1 + 0.91X)^{1/2}. \quad (1)$$

The mixing depth has no effect at small X except through the term w^*, because $X = (x/U)w^*/z_i$. The small X asymptote, $\sigma_y = 0.51w^*(x/U)$, is consistent with the small-x statistical theory asymptote, $\sigma_y = \sigma_v t$, and the approximations $t = x/U$ and $\sigma_v \propto w^*$; the latter holds through almost the whole mixing layer in moderately to very convective conditions. The large X asymptote, $\sigma_y = 0.53(w^* z_i x/U)^{1/2}$, implies an effective lateral eddy diffusivity equal to $0.14w^*z_i$. This type of diffusion would result from any "random walk" with velocities scaling to w^* and lateral displacements scaling to z_i, provided that $\sigma_y \gg z_i$. Equation (1) was based on vertically-integrated χ from the first tank experiments of Willis and Deardorff (1976a), with $z_s/z_i = 0.067$. However, in the atmosphere, flow structures on scales larger than z_i often cause wind direction shifts on time scales larger than z_i/U; these would cause increased growth of σ_y, with a larger exponent than ½ in x.

Lamb (1979) suggested parameterizations for σ_y that approximately fit his numerical modeling results. He

divided these into two cases, one fitting the near-surface release ($z_s/z_i = 0.026$) and one fitting the elevated-release numerical runs ($z_s/z_i = 0.26$, 0.52, and 0.74). Note the larger growth in σ_y at small X for the near-surface case; this might result from diverging flow near the base of downdrafts, a consequence of continuity and the suppression of vertical motion by the surface.

$$\left.\begin{aligned} \text{Near-surface:}\quad \sigma_y/z_i &= 0.6X \quad \text{at} \quad X \leqslant \tfrac{1}{6}, \\ &= \left(\tfrac{1}{3}\right)X^{2/3} \quad \text{at} \quad X > \tfrac{1}{6} \\ \text{Elevated:}\quad \sigma_y/z_i &= \left(\tfrac{1}{3}\right)X \quad \text{at} \quad X \leqslant 1, \\ &= \left(\tfrac{1}{3}\right)X^{2/3} \quad \text{at} \quad X > 1 \end{aligned}\right\}. \quad (2)$$

Nieuwstadt (1980) tested the Deardorff and Willis (1975) parameterization, Eq. (1), against the Prairie Grass field data. These consisted of near-surface measurements of σ_y from a near-surface source, at distances from 50 to 800 m (nondimensional X ranging from 0.01 to 2). Nieuwstadt noted that the field values of σ_y were generally larger than σ_y from Eq. (1), and that the best fit would be given by Eq. (1) times a factor 1.4. A similar conclusion could be made from the collection of field-measured values (including Prairie Grass) plotted in Briggs (1985). This plot is shown here in Fig. 1, along with a suggested fit to the bulk of the data:

$$\sigma_y/z_i = 0.6X/(1 + 2X)^{1/2}. \quad (3)$$

This approximates all the data except for two cases: 1) Run 1 of Prairie Grass (flagged), which had two peaks in the lateral distribution of concentration, probably caused by a wind shift, and 2) two BAO runs made

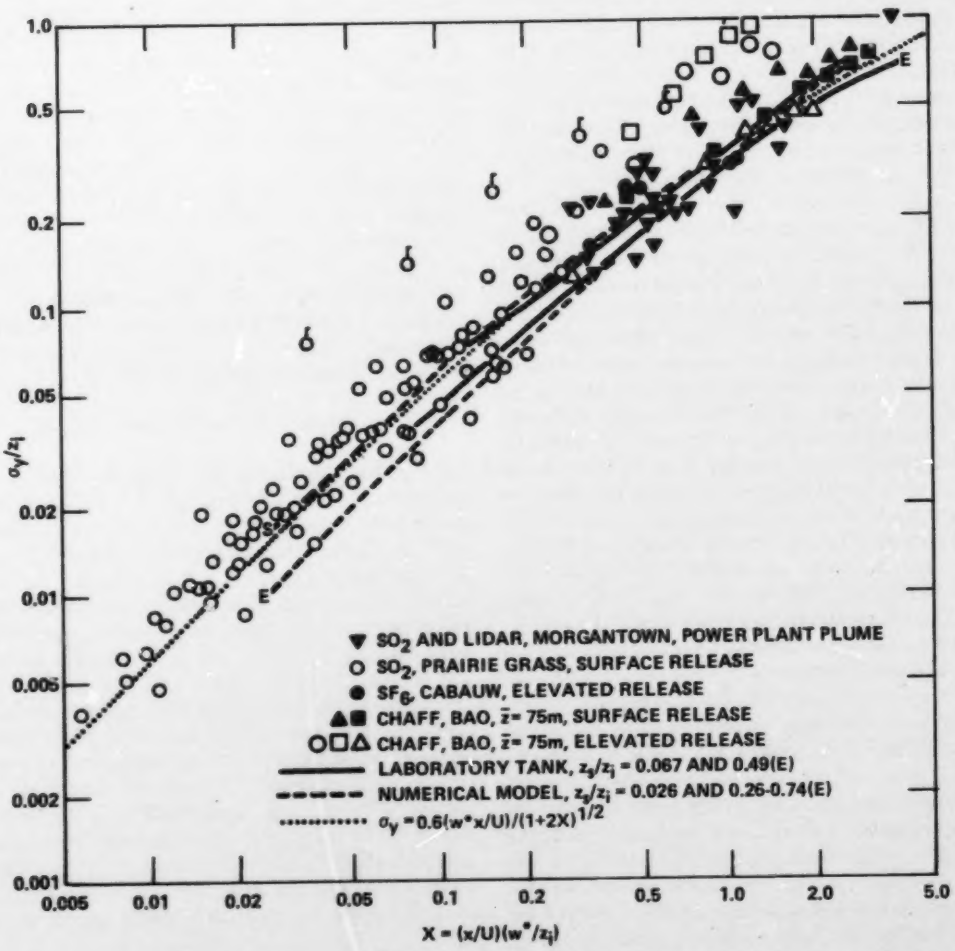

FIG. 1. Lateral dispersion, nondimensionalized by z_i, vs $X = (x/U)w^*/z_i$. "E" indicates elevated source releases; other data lines are near-surface releases. Flagged circles are Prairie Grass run 1, double peak in χ vs y.

consecutively on a day with large wind direction shear in the mixed layer; in these cases, σ_y is 2 or 3 times as large. Thus, Eq. (3) might be regarded as a minimum σ_y estimate for the CBL; it does give 80% larger σ_y than Lamb (1979) found for elevated sources at small X, but at the distance of maximum surface impact from the elevated sources, the difference between Eqs. (2) and (3) is less than 25% (they agree at $X = 2.4$). The form of Eq. (3) is similar to that of Eq. (1) (Deardorff and Willis, 1975), but Eq. (3) is larger by 18% at small X and is smaller by 21% at large X.

Because these parameterizations and the data they are based on indicate a slow drop-off from a linear relationship in x, several modelers have simply used linear relationships as approximations for σ_y for use in models of diffusion from elevated sources. Venkatram and Vet (1981) suggested $\sigma_y = 0.45(w^*/U)x$, finding that it gave just as accurate predictions of surface concentrations from very buoyant, elevated sources as the more complex expression of Venkatram (1980), within the range of the tested data. Misra (1982) made a similar approximation, $\sigma_y = 0.4(w^*/U)x$, apparently as a rough fit to Willis and Deardorff's (1978) observations for their $z_s/z_i = 0.24$ source in a limited range of X. It overpredicts most σ_y observations shown here in Fig. 1 by 50% or more at $X \geq 2$, but deviates from Eq. (3) by less than 20% in the range $0.2 < X < 1.2$.

Several parameterizations for σ_y that include both convective and neutral boundary layer limits have been suggested. At small x or t, these are linear, with $\sigma_y \propto w^*t$ (or $\sigma_y/z_i \propto X$) in the purely convective case and $\sigma_y \propto u^*t$ in the purely neutral case. The latter approximation follows from the assumption that σ_v/u^* is constant in neutral conditions. Experimentally, this constant ranges from about 1.5 to 3 at different sites, and may be influenced by mesoscale features of the terrain (Panofsky, 1973). The convective asymptote, with σ_v/w^* a constant, shows less variability from site to site. We find some observational trend in this ratio with $|z_i/L|$ [which equals $k(w^*/u^*)^3$], but for practical purposes $\sigma_v/w^* \approx 0.6$ fits observations within $\pm 15\%$ when $|z_i/L| > 10$ or so (this approximation includes 90% of the points shown in Fig. 1 of Panofsky *et al.* (1977). A simple formulation which bridges the neutral and convective asymptotes was suggested by Weil and Brower (1982):

$$\sigma_y = \frac{[(0.56w^*)^2 + (1.6u^*)^2]^{1/2}t}{[1 + x/(10\text{ km})]^{1/2}}. \quad (4)$$

The convective asymptote is a fit to the analysis of the 1973 Minnesota boundary layer experiment by Kaimal *et al.* (1976), applicable to the upper 90% of the mixing layer. The neutral asymptotes, as well as the universal function of x in the denominator, are adopted from the empirical parameterizations suggested by Briggs (Gifford, 1975); these were merely approximate fits to Pasquill's (1961) σ_y curves in the range $x = 0.1$ to 10 km (caution: these curves apply to only 3-min averaging periods). A more complex, and more completely physical, formulation was given by Nieuwstadt and Van Duuren (1979):

$$\left.\begin{aligned} \sigma_y &= [(0.51w^*)^3 + (1.7u^*)^3]^{1/3}t/[1 + t/t_i]^{1/2} \\ t_i &= h/[(0.91w^*)^3 + (2.5u^*)^3]^{1/3} \\ h &= z_i \text{ or } 0.3u^*/f \end{aligned}\right\}. \quad (5)$$

These equations were developed from Deardorff and Willis's (1975) σ_y equation for the convective case; the constants for the w^* terms are taken from this earlier result, Eq. (1) in this paper. The small t asymptote for the neutral case, $\sigma_y = 1.7u^*t$, comes from $\sigma_y \approx \sigma_v t$ and an empirical fit to turbulence data at source height at Cabauw in neutral conditions, $\sigma_v/u^* = 1.7$. The constant for the u^* term in the expression for t_i is obtained by equating the neutral form of t_i, with $w^* = 0$ and $h = 0.3u^*/f$ (Tennekes, 1973), with Draxler's (1976) empirical fit to σ_y observations, $t_i = 1200$ s. One might select $h = 0.3u^*/f$ when z_i is undefinable, in which case w^* is also undefinable; alternatively, one might use it when $0.3u^*/f > z_i$. Nieuwstadt and Van Duuren do not make a clear recommendation here, although they show a good comparison of Eq. (5) with the Cabauw observations (Agterberg *et al.*, 1983). One approach that would be consistent with their σ_y and t_i expressions, at least, is

$$h = [z_i^3 + (0.3u^*/f)^3]^{1/3}. \quad (6)$$

Enhanced σ_y growth due to buoyant plume rise is included in several modeling parameterizations in the literature. These are cast in terms of convective scaling; thus, they involve a new dimensionless parameter that includes the buoyancy per unit length of bent-over plume, F_b/U: $F^* = F_b/(Uw^{*2}z_i)$. For effluent of molecular weight similar to air, F_b is $g/(\pi\rho c_p T)$ times the rate of sensible heat emission, Q_H (Briggs, 1984) (g is gravity, ρ ambient air density, and c_p specific heat capacity of air); F_b is typically of the order 1000 $m^4\ s^{-3}$ for a large power plant. Roughly, F^* compares the buoyancy in a horizontal segment of plume of length z_i, $F_b(z_i/U)$, to the buoyancy of an average ambient thermal, $z_i^2H^*(z_i/w^*)$. Weil (1979) used Lamb's (1979) expression for a passive, elevated source and combined it using vectorial addition with buoyant plume expansion due to entrainment in its rising state; the latter is given by the "⅔ law" for buoyant plumes, width $\propto$ rise $\propto F_b^{1/3}U^{-1}x^{2/3}$. Weil's result for single-stack plumes is

$$\begin{aligned} \sigma_y/z_i &= \left(\frac{1}{3}\right)X[1 + 7.3(F^*/X)^{2/3}]^{1/2} \quad \text{at} \quad X \leq 1 \\ &= \left(\frac{1}{3}\right)X^{2/3}[1 + 7.3F^{*2/3}]^{1/2} \quad \text{at} \quad X > 1. \end{aligned} \quad (7)$$

Venkatram (1980) made similar assumptions about σ_y, except that he based his passive plume component on

a fit to the data of Willis and Deardorff (1976a). Recasting his result in a form similar to Eq. (7), we have

$$\sigma_y/z_i = 0.45X[1 + 1.57(F^*/X)^{2/3}]^{1/2} \quad \text{at} \quad X \leq 1$$
$$= 0.45X^{2/3}[X^{0.4} + 1.57F^{*2/3}]^{1/2} \quad \text{at} \quad X \geq 1. \tag{8}$$

Venkatram's initial passive plume growth is a factor 1.35 times Weil's, and the power law in X in Eq. (8) is somewhat larger for $X > 1$, $X^{0.86}$ instead of $X^{0.67}$; in contrast, Venkatram's buoyant growth term is a factor 1.6 smaller.

An analysis of buoyant plume data that was added to this paper in revision indicates that neither Eq. (7) nor (8) gives an entirely satisfactory fit to the Dickerson and Morgantown power plant *surface* σ_y observations. The large F^* asymptote is roughly 80% larger than in Eq. (7) and 180% larger than in Eq. (8). The onset of F^* effects on σ_y is more abrupt than is given by the F^* terms of these two equations, and there are no obvious F^* trends at $F^* < 0.03$. For small F^* cases, these power plant surface observations are fit best by Eq. (7) [with $F^* = 0$, so that it reverts to Eq. (2)] times a factor of 1.5.

4. Parameterizations for σ_z

Many models use the conventional Gaussian assumption for vertical concentration distribution, with an analytical form for σ_z. As will be seen in the conclusion, this approach may be more successful with buoyant plumes than with passive plumes. However, in some applications satisfactory results can be obtained for passive sources; these are mentioned in the penultimate paragraph of this section.

Deardorff and Willis (1974, 1975) suggested a σ_z parameterization for the purely convective case in 1974, but the parameterization of 1975 is more physically reasonable ($d\sigma_z/dt$ increases with source height in the layer below $0.5z_i$, for instance). The 1975 parameterization also includes mechanical turbulence effects, using u^*. If we neglect the u^* term in their equation for σ_z, we have $\sigma_z/z_i = X[1.8Z_s^{2/3} + 0.25X]^{1/2}$, where $Z_s = z_s/z_i$. The first term satisfies Taylor's short-range formula, $\sigma_z = \sigma_w t$, with $\sigma_w = 1.34(H^* z_s)^{1/3}$, as recommended by Wyngaard *et al.* (1971) for the surface layer. The second term satisfies Yaglom's (1972) free convection formula, $\sigma_z \propto H^{*1/2} t^{3/2}$, with the constant supplied from the tank experiments. This equation is valid only when $X \leq 0.5$, since the vertical concentration distribution in the tank experiments became markedly non-Gaussian at slightly larger distances. Lamb (1979) also offered σ_z equations, as well as the σ_y equations given here as Eqs. (2), for the purely convective case. These were based on his numerical experiment with particle trajectories:

$$\left.\begin{aligned} \text{Near-surface:} \quad \sigma_z'/z_i &= 0.5X^{1/2} \quad \text{at} \quad X \leq 1.2, \\ &= 0.6 \quad \text{at} \quad X > 1.2 \\ \text{Elevated:} \quad \sigma_z'/z_i &= 0.5X \quad \text{at} \quad X \leq \tfrac{2}{3}, \\ &= \tfrac{1}{3} \quad \text{at} \quad X > \tfrac{2}{3} \end{aligned}\right\}. \tag{9}$$

These equations are not fits to Gaussian plumes, since the plumes became non-Gaussian, just as in the tank experiments; rather, $\sigma_z'^2$ is defined by $\overline{(z_p - z_s)^2}$, where z_p is the height of a particle. The asymptotic value of σ_z'/z_i for uniform mixing between $z = 0$ and z_i is $[\frac{1}{3} - Z_s + Z_s^2]^{1/2}$, which is 0.58 for $Z_s = 0$ or 1, 0.38 for $Z_s = \frac{1}{4}$ or $\frac{3}{4}$, and 0.28 for $Z_s = \frac{1}{2}$; Lamb's asymptotes are therefore approximate. Note the empirical exponent in X for the near-surface release in the growth stage, between 1 and $\frac{3}{2}$; source height effects are not explicitly included in this parameterization, but instead are broadly categorized.

Several σ_z parameterizations include both convective and neutral limits. Deardorff and Willis's (1975) full equation is

$$\left.\begin{aligned} \sigma_z/z_i &= X[1.8Z_s^{2/3} + 0.25X + (b'u^*/w^*)^2]^{1/2} \\ b' &= [0.8 + 0.4(u^*/U)x/z_s]/[1 + (u^*/U)x/z_s] \end{aligned}\right\}. \tag{10}$$

The b' term replaces w^* (implicit in X) with u^*, providing a term for σ_z growth due to mechanical turbulence, which becomes the neutral asymptote when w^* vanishes. The sliding constant, b', is meant to adjust between early results for surface plumes, $\sigma_z = 0.4u^*t$, and the short-time (small $(x/U)u^*/z_s$) Taylor prediction $\sigma_z = \sigma_w t$ using $\sigma_w = 1.2u^*$ (to be consistent with this, 0.8 should be 1.2 in the expression for b'; however, it is written here as it appeared in the 1975 reference).

For a surface source, Eq. (10) gives $b' = 0.4$. A somewhat larger constant for the u^* term is suggested in Eq. (15) of Briggs (1982), based on an analysis of the Prairie Grass field data. This equation is written in terms of crosswind-integrated concentration at the surface, $\int \chi_0 dy$, because this quantity was measured directly. If we restrict our application to $X \leq 0.5$, as Deardorff and Willis (1975) stipulate, then we can assume a nearly Gaussian plume, for which $\sigma_z = (2/\pi)^{1/2}Q/(U\int \chi_0 dy)$. Then the Briggs (1982) equation can be rewritten as

$$\sigma_z/z_i = X[0.53X + (0.64u^*/w^*)^2 + \text{sweepout}]^{1/2}. \tag{11}$$

The "sweepout" term, proportional to X^3, is omitted here because it mostly reflects the non-Gaussian stage of plume growth. In Briggs (1982), the constant for the free convection term is $0.027U_g/u^*$; the ratio U_g/u^* is an artifact of the simplified, approximate scaling scheme that was employed, and should not appear in convective scaling; Prairie Grass values of U_g/u^* varied

less than 10% from their average value, 19.4, so this has been substituted to get the constant 0.53 in Eq. (11). Thus, the constant for the free convective asymptote in this equation, $(0.53)^{1/2} = 0.73$, is larger than that in Deardorff and Willis (1975), $(0.25)^{1/2} = 0.50$. However, when they did not include a Z_s term, Deardorff and Willis (1974) fit their tank observations with $\sigma_z/z_i = 0.84X^{3/2}$. This is close to the free convection asymptote that Nieuwstadt (1980) fit to the Prairie Grass data, $C_y = 0.9X^{-3/2}$, if one makes the Gaussian assumption $\sigma_z/z_i = 0.8/C_y = 0.89X^{3/2}$, where $C_y = z_iU \times \int \chi_0 dy/0$. I conclude that the consistency between the tank and Prairie Grass observations is acceptable for the free convective regime, but that the field observations indicate a considerably larger neutral limit, $\sigma_z = 0.64u^*t$.

The convective–neutral σ_z parameterization of Weil and Brower (1982) is intended for use in elevated source models:

$$\sigma_z/z_i = X[(0.56)^2 + (1.26u^*/w^*)^2]^{1/2}. \quad (12)$$

This is based on the short-range approximation, $\sigma_z = \sigma_w t$. For the convective limit, $\sigma_w/w^* = 0.56$ is a best fit to the 1973 Minnesota boundary layer measurements reported by Kaimal *et al.* (1976) for $z/z_i > 0.1$. The neutral limit, $\sigma_w/u^* = 1.26$, is taken from Panofsky *et al.* (1977). Both of these limits are supported, at least approximately, by the bulk of available, appropriate measurements. This σ_z growth rate must slow somewhat as the plume approaches the ground (i.e., as σ_z approaches the effective source height) or if the top of the plume impinges on z_i. However, the greatest uncertainty in elevated source models for the CBL is in the effective source height, rather than in σ_z.

One way to reconcile the differences between Eqs. (10), (11), and (12) is the following. For a near-surface source, use Deardorff and Willis's (1975) formula, Eq. (10), only multiply their b' value by a factor of 1.6. For large $X'' = (u^*/\bar{U})x/z_s$, it would then essentially agree with the Briggs (1982) analysis of Prairie Grass, and at small X'' the u^* term would nearly equal Weil and Brower's (1982) u^* term, for a plume still elevated. For a sufficiently elevated source, use Eq. (12). A crossover point is given by equating the convective terms of Eqs. (10) and (12) at small X, $1.8Z_s^{2/3} = (0.56)^2$; therefore, use Eq. (10) if $Z_s < 0.07$, and Eq. (12) if $Z_s > 0.07$. However, keep in mind the non-Gaussian behaviors observed of passive plumes. If Eq. (10) is used in a conventional Gaussian model, it can be expected to overpredict ground concentration in the range $0.7 < X < 3$, approximately, for low-level, passive sources. For elevated, passive sources, Eq. (12) used in this manner can be expected to underpredict the peak ground concentrations by a factor approximating $(1 + 2Z_s)$, with improving agreement with observations at distances beyond the peak. Alternative parameterizations which are in better agreement with passive plume observations are given in the next section. Figure 2 shows a comparison of Eqs. (9)–(12).

For elevated plumes with buoyancy, Weil and Brower (1982) adopted the suggestion of Pasquill (1976), using vectorial addition of σ_z for passive plumes (Eq. (12)) and $\sigma_z = \Delta h/3.5$, where Δh is the calculated final plume rise due to buoyancy. Venkatram (1980) suggested

$$\sigma_z/z_i \approx 1 - e^{-(X+F^{*1/3}X^{2/3})}$$

$$F^* = F_b/(Uw^{*2}z_i) \quad (13)$$

which amounts to linear addition at small X of a passive term, X, and a buoyancy-induced growth term, $F^{*1/3}X^{2/3}$; this term is consistent with growth proportional to plume rise in the "⅔ law" regime, $\Delta h \propto F_b^{1/3}U^{-1}x^{2/3}$. The numerical coefficients of these terms, all unity, are about 1.5 times most estimates. Nevertheless, when used in Venkatram's complete model for ground concentrations from elevated, buoyant plumes, which also contains impingement and σ_y assumptions, it gives approximately correct magnitudes, as compared to observations at two power plants. A later, simplified version of this model uses even more rapid passive growth of σ_z, while eliminating the buoyancy-induced growth: $\sigma/z_i = 1 - \exp(-1.5X)$, where σ is defined as "vertical spread" and functions just as σ_z usually does in a concentration equation (Venkatram and Vet, 1981). I would like to add that, in practice, buoyancy-induced vertical dispersion does not seem to be important to modeling concentration exposures, unless a plume impacts on elevated terrain or objects close to the source.

5. Surface $\int \chi dy$ parameterizations

The laboratory tank simulations of Willis and Deardorff, the numerical modeling experiments of Lamb, and the full-scale experiments at the Boulder Atmospheric Observatory all indicate highly non-Gaussian diffusion in the vertical dimension in the CBL. Therefore, conventional Gaussian models, even with optimum parameterizations for σ_y and σ_z, may give unsatisfactory results for surface concentrations. Briggs (1985) concluded from the above experiments that the maximum surface value of crosswind-integrated concentration, $\int \chi_0 dy$ is enhanced for passive sources by a factor $\approx(1 + 2z_s/z_i)$ over that predicted by the Gaussian model, $(\int \chi dy)_{max} = (2/\pi e)^{1/2}Q/(Uz_s)$. This result occurs at $\sigma_z = z_s$, and is unaffected by the form chosen for σ_z versus x. The Gaussian plume model could be altered to give this result, e.g., by simply centering the plume at an effective source height $h_e = z_s/(1 + 2z_s/z_i)$. More realistically, we could assume a descent of the plume axis from z_s, Δz, that is proportional to σ_z. Setting $\Delta z/\sigma_z = 2A$, we find that the maximum $\int \chi dy$ is enhanced by a factor $[A + (1 + A^2)^{1/2}]$ times $\exp[A(-A + (1 + A^2)^{1/2})]$. This closely approximates

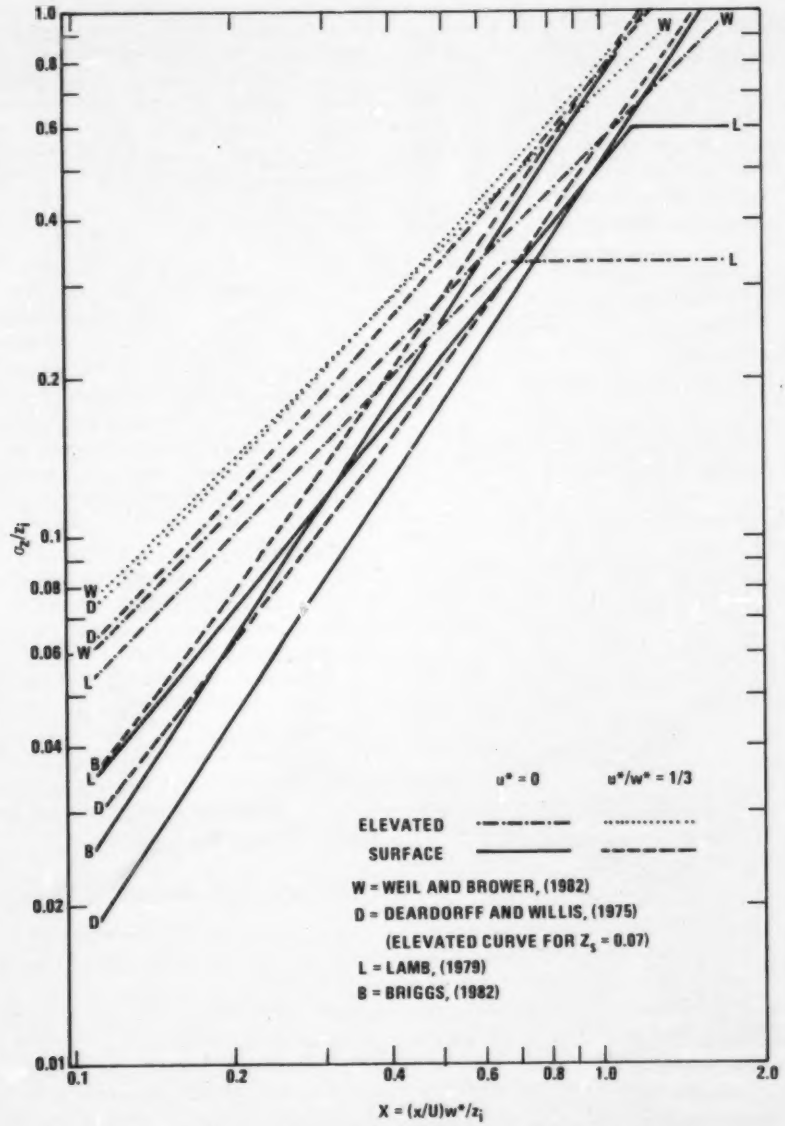

FIG. 2. Vertical dispersion, nondimensionalized by z_i, vs $X = (x/U)w^*/z_i$, various parameterizations.

the $(1 + 2z_s/z_i)$ observed enhancement if we set $A = Z_s/(1 + 0.3Z_s)$, where $Z_s = z_s/z_i$.

An alternative is to forget about the vertical distribution of concentration and attempt to parameterize only the surface value of $\int \chi dy$. This parameterization could be based on an altered Gaussian plume concept, or could be more directly empirical. Since observed lateral distributions of average plume concentration are roughly Gaussian, we can retrieve the surface concentration from

$$\chi = \frac{\int \chi dy}{(2\pi)^{1/2}\sigma_y} e^{-0.5(y/\sigma_y)^2}. \quad (14)$$

A model suggested by Venkatram in 1980 was designed to predict only ground level concentrations for elevated, buoyant sources. It gave good fits to observed ground concentrations for two power plants reported by Weil (1977). The model was based on the propo-

sition that downdrafts of velocity $\approx 0.5w^*$ cause surface impact of the plume at $x = \bar{x}_i$, on the average, with

$$h_s + 1.0F_b^{1/3}U^{-1}\bar{x}_i^{2/3} - 0.5w^*\bar{x}_i/U = 0 \quad (15)$$

where h_s is the actual, rather than the effective, source height. It is assumed that the plume is totally on the ground beyond some impact x_i, with a ground source equation being appropriate, and totally off the ground at lesser x, with a Gaussian distribution of $\ln(x_i/\bar{x}_i)$ about $x_i = \bar{x}_i$ and a standard deviation in x_i of a factor of 2. The particular forms chosen for σ_y and σ_z are given here by Eqs. (8) and (13), respectively. The result for dimensionless crosswind-integrated surface concentration is

$$C_y = (\sigma_z/z_i)^{-1}f(x) \quad (16)$$

where $f(x) = (2\pi)^{-1/2}\int_{-\infty}^{p} e^{-q^2/2}dq$ and $p = \ln(x/\bar{x}_i)/\ln 2$. This model could be applied to non-buoyant sources; however, compared to Willis and Deardorff's (1978, 1981) and Lamb's (1979) results for $Z_s = \frac{1}{4}$ and $\frac{1}{2}$, it predicts a peak in C_y about a factor of 2 too small. Part of this may be because Eq. (13) gives too rapid an initial growth in σ_z. A modified version of this model (Venkatram and Vet, 1981) assumes even more rapid σ_z growth, while reducing the spread of impact points somewhat, replacing ln2 with ln1.5 for a passive source. Either of these versions appears to perform well when compared to tested data from large, buoyant sources, but underpredicts peak C_y for passive sources.

Another class of convective vertical diffusion models for elevated sources is represented by Weil and Furth (1981), Misra (1982), and Venkatram (1983). These all use the probability distribution of vertical velocities at source height, which has a negative mode in the CBL, to account for the downward trend of the centerline of maximum concentration. Essentially, they all assume an infinite or very long Lagrangian time scale, so that near the source, before any reflection occurs,

$$\int \chi dy = Qp(w_0|z_s)/x \quad (17)$$

where $p(w|z)$ is the probability of vertical velocity w per small increment in w at height z, and $w_0 = u(z - z_s)/x$; p has units of inverse velocity and satisfies $\int_{-\infty}^{\infty} pdw = 1$. The models make different assumptions about the form of p, reflection characteristics, and about the effects of z on particle trajectory vertical velocities. Misra assumed that w for a particle trajectory is proportional to $(z/z_i)^{1/3}(1 - 1.1z/z_i)$, after Lenschow and Stevens (1980). In the other two models, w for a particle trajectory is assumed constant in between reflections. Misra and Venkatram both assumed simple reflection at the surface, with the direct contribution to χ doubled; Venkatram also included such a reflection at z_i, in the form of a virtual source at $x = 0$, $z = 2z_i - z_s$. In contrast, Weil and Furth assumed that when a particle reflects, its absolute velocity changes in proportion to the ratio of mean updraft and mean downdraft velocities, $\bar{w}_u$ and $\bar{w}_d$, respectively. Guided by Lamb's (1978, 1979) results, they assumed $\bar{w}_u = 0.6w^*$ and $\bar{w}_d = 0.4w^*$, so that $\bar{w}_u/\bar{w}_d = 1.5$. One consequence of this speed change during reflection is that concentration reflected from the surface is $\frac{2}{3}$ of the direct concentration impacting the surface, and the concentration reflected from z_i is $\frac{3}{2}$ of the direct concentration impacting z_i; another way to account for this is with virtual sources at $x = 0$ and $z = -(\frac{3}{2})z_s$, $z = z_i + (\frac{2}{3})(z_i - z_s)$, with probability distributions $p_v(w > 0) = (\frac{2}{3})p[-(\frac{2}{3})w]$ and $p_v(w < 0) = (\frac{3}{2})p[-(\frac{3}{2})w]$.

Weil and Furth (1981) also assumed different fractional areas for updrafts and downdrafts, A_u and A_d, respectively, with $(A_u + A_d) = 1$ and $A_d/A_u = \bar{w}_u/\bar{w}_d = 1.5$, consistent with Lamb's results and $\bar{w} = 0$. Thus, the rate of emission is divided into an initially downdrafted portion, $A_dQ = 0.6Q$, and an initially updrafted portion, $A_uQ = 0.4Q$. Curiously, the sum of direct and reflected concentrations at the surface is not affected by A_d/A_u; the initially downdrafted Q is multiplied by the factors $A_d(1 + w_d/w_u) = A_d(1 + A_u/A_d) = 1$, and the initially updrafted Q is multiplied by the factors $A_u(1 + \bar{w}_u/\bar{w}_d) = A_u(1 + A_d/A_u) = 1$. Weil and Furth assumed a probability distribution function of the form $P = \eta e^{-\eta}$ for both updrafts and downdrafts, where $\eta = |\bar{w}/(0.5w)|$ in each case (in the 1981 reference, "0.5" appears in the numerator of the definition of η; however, in order that $\bar{w} = \int_0^\infty |w|Pd\eta/\int_0^\infty Pd\eta$, 0.5 should be in the denominator). When we add the requirement that $\int_0^\infty pd|w| = 1$, we finally get $p = (2/\bar{w})P$ for both updrafts and downdrafts, with $\bar{w} = \bar{w}_u$ or $\bar{w}_d$, respectively. Weil and Furth (1981) solved this model in Monte Carlo fashion by releasing 4000 particles of random velocity shaped by $P(\eta)$ into a numerical grid, allowing any number of reflections to occur. However, analytic solutions can be derived from the stated assumptions. Including a direct term $(w = -uz_s/x)$, a single reflection from $z_i\{w = u[(\frac{5}{2})z_i - z_s)/x]\}$, and a reflection from both $z = 0$ and $z_i\{w = -u[(\frac{5}{3})z_i + z_s)/x]\}$, we find that

$$X^2C_y = a^2Z_se^{-aZ_s/X} + b^2Z_1e^{-bZ_1/X} + a^2Z_2e^{-aZ_2/X} \quad (18)$$

where $a = 2/0.4 = 5$, $Z_1 = (\frac{5}{2} - Z_s)$, $b = 2/0.6 = \frac{10}{3}$, and $Z_2 = (\frac{5}{3} + Z_s)$. This equation closely agrees with the Monte Carlo simulation for $Z_s = 0.26$, except that it is smoother in X. It should be accurate up to $X \approx 4$, beyond which further reflections may substantially contribute; however, the vertical distribution of concentration is nearly uniform in this case, so $C_y \approx 1$.

Misra (1982) also assumed $A_d = 0.6$ for a particular case, $Z_s = 0.24$. He assumed a double Gaussian form for p, i.e., Gaussian downdrafts and Gaussian updrafts. For the downdrafts, he estimated $\bar{w}_d = 0.11w^*$ and σ_w

$= 0.37w^*$; these were assumed the only significant contributors to peak surface concentrations. He arbitrarily set the "surface" at $z = z_i/40$, to avoid a singularity at $z = 0$ due to the assumed form for w versus z (it would be more consistent with Misra's Eq. (17) to consider the surface at $z/z_i = (u^*/w^*)^3 = -kL/z_i$; however, this adds considerable complexity). For $Z_s = 0.24$, Misra's result is

$$XC_y = 2.07e^{-(0.46/X-0.21)^2}. \tag{19}$$

Contributions from reflection at z_i are modeled quite differently, and probably are not significant until $X > 2$. Equation (19) is quite similar to the "descending Gaussian plume" model for constant $\Delta z/\sigma_z$ described in the opening paragraph of this section, with $\Delta z/\sigma_z = \bar{w}_d/\sigma_w = 0.30$. It differs primarily in that C_y is multiplied by the factor 0.6, for only the downdraft portion of Q, and by 1.61, a consequence of the slowing of w near the surface.

The "bouncing ball" model proposed by Venkatram (1983) is relatively straightforward, with

$$XC_y = 2[w^*p(w_1|z_s) + w^*p(w_3|z_s)] \tag{20}$$

where $w_1 = -Uz_s/x$ and $w_3 = U(2z_i - z_s)/x = (1 - 2/Z_s)w_1$. However, he used a graphical form of p, the curves for $Z_s = 0.24$ and 0.49 that were derived by Lamb (1981) from numerical modeling. In order to provide a completely analytic form for this method, I offer the following suggestion for p as a function of $W = w/w^*$:

$$\left.\begin{aligned} W > 0, \quad w^*p &= 0.5 \exp -(0.9W + 0.1W^4) \\ W < 0, \quad w^*p &= 0.5 \exp -(0.9W + 1.8W^4) \end{aligned}\right\}. \tag{21}$$

This function fits both of Lamb's curves within ±5% of the peak value of w^*p for negative W, and closely approximates the curve for $Z_s = 0.49$ for positive W (the poorer fit to w^*p for $Z_s = 0.24$, $W > 0$, is not significant until $X > 1.5$ or so, when the reflection from z_i term (w_3) noticeably contributes).

A model with the simplicity of Eq. (20) could be made to give excellent fits to C_y versus X data by choosing an "effective" p which produces the desired agreement. We would probably find that w^*p must be a function Z_s, as well as W, as Lamb and others find is the case for w distribution [Eq. (21) is a compromise between w^*p for $Z_s = 0.24$ and for $Z_s = 0.49$]. It is also possible to develop C_y equations which are entirely empirical fits to laboratory, numerical, or field data. I have done this using the laboratory results of Willis and Deardorff (1976a, 1978, 1981), for $Z_s = 0.067$, 0.24, and 0.49. The equation is

$$C_y = \frac{0.9(X/Z_s)^{9/2}}{[1 + 0.4(X/Z_s^{5/6})^{9/2}]^{4/3}} + \frac{1}{[1 + 3Z_s^{1/2}X^{-3/2} + 50X^{-9/2}]}. \tag{22}$$

The first term dominates at $X < 1.5$, approximately. It has a rapid rise stage with $C_y = 0.9(X/Z_s)^{9/2}$ and a falling stage with $C_y = 3Z_s^{1/2}X^{-3/2}$. The peak C_y, which occurs at $X = 1.56Z_s^{5/6}$, is $1.06Z_s^{-3/4}$. This matches the simple Gaussian model prediction, peak $C_y = 0.484Z_s^{-1}$ at $\sigma_z = z_s$, at $Z_s = 0.043$. Therefore, Eq. (22) gives an enhancement in peak concentration $\propto Z_s^{1/4}$ compared to the Gaussian model, but should not be used for $Z_s \leq 0.04$. The second term brings C_y up to its uniform vertical mixing asymptote, $C_y = 1$, after an "undershooting" stage during which most of the tracer was in the upper half of the laboratory tank mixing layer.

Figure 3 shows a comparison of Eq. (22) with Willis and Deardorff's laboratory results. The Gaussian model, recommended for $Z_s < 0.04$, is shown also, with $h_e = z_s$ and the pure convective form of Eq. (10) for σ_z:

$$\sigma_z/z_s = XZ_s^{-2/3}(1.8 + 0.25XZ_s^{-2/3})^{1/2}.$$

In order to show this "base case" as a single curve independent of Z_s, Fig. 3 is plotted as $Z_sC_y = z_sU \times \int \chi_0 dy/Q$ versus $XZ_s^{-2/3}$. The Gaussian model curve is not valid at $X > 1.5$, when reflection from z_i becomes significant. This figure shows a good fit of the laboratory results with Eq. (22); this equation facilitates interpolation or extrapolation to any value of Z_s. It also shows the clear trend towards larger peak (Z_sC_y) with increasing Z_s, evidently a consequence of the reponderance of downdraft area in the mid-mixing layer. For comparison, the peak $(Z_sC_y) \approx 1 + 2Z_s$, occurring at $X \approx 2Z_s$, suggested by Briggs (1985), is shown with triangles.

Figure 4 shows a comparison of the Weil and Furth (1981), Misra (1982), and Venkatram (1983) models with Willis and Deardorff's (1978, 1981) laboratory results and Lamb's (1979) numerical results, for $Z_s = ¼$ and $Z_s = ½$, separately. The Venkatram (1980) model is not shown, since it considerably underpredicts the peak C_y for passive sources and lacks the pronounced peak in the shape of C_y versus X seen in the experimental results. We see in Fig. 4a that Weil and Furth's model gives a good fit to Lamb's curve for $Z_s = 0.24$, as was shown in their paper, but for $Z_s = 0.52$ (Fig. 4b) the peak in C_y is too small and a bit late, in terms of X. The main weakness of this model is probably the particular choice for $p(w|z)$, which unrealistically approaches zero at small $|w|$ and drops off comparatively slowly at large $|w|$. Misra's model gives a reasonably satisfactory fit for the $Z_s \approx ¼$ case, but needs adaptability to other Z_s. The analytic form for w^*p in Eq. (21) is seen to provide a good approximation to Venkatram's (1983) results, which use a graphical w^*p. This model provides a rather good fit to the peak values of C_y, especially for the tank data, but the peaks occur at X values that are too small by a factor of ~0.7.

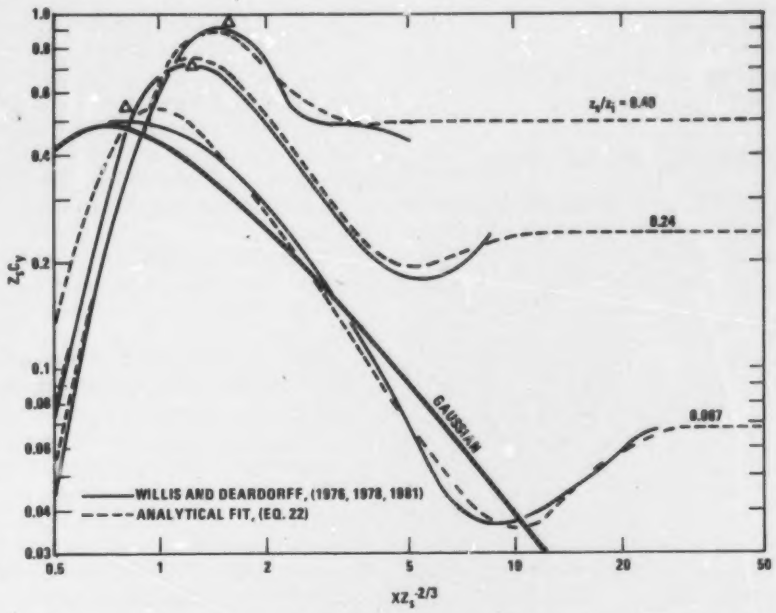

FIG. 3. Crosswind-integrated, near-surface concentration, nondimensionalized as $Z_sC_y = z_iu \int \chi dy/Q$, vs $XZ_s^{-2/3}$, where $Z_s = z_s/z_i$. "Gaussian" curve is Gaussian model calculation with σ_z given by $\sigma_z/z_s = XZ_s^{-2/3}(1.8 + 0.25XZ_s^{-2/3})^{1/2}$. Triangles are peaks given by $Z_sC_y = 1 + 2Z_s$, $X = 2Z_s$ (Briggs, 1985).

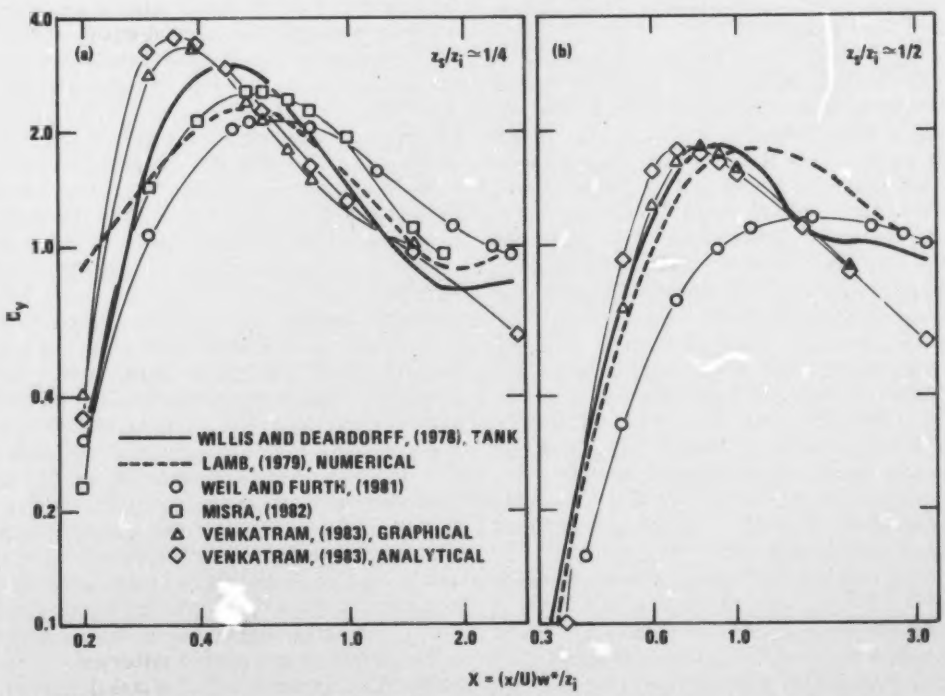

FIG. 4. Crosswind-integrated, near-surface concentration, nondimensionalized as $C_y = z_iU \int \chi dy/Q$, vs $X = (x/U)w^*/z_i$, for laboratory tank experiments, numerical experiments, and various parameterizations.

As Venkatram pointed out, this would be an expected consequence of downward motions slowing down as the surface is approached; the model simplistically assumes straight line trajectories.

6. Further considerations on buoyant plumes

One reviewer of the first draft of this paper requested a clearer recommendation on modeling of buoyant plumes. There are the options of using an experiment-based passive plume formulation for C_y or of using a Gaussian model with a σ_z parameterization; the latter gives a less pronounced peak for C_y, $Z_s C_y = 0.484$. Both approaches require a plume rise calculation to evaluate $Z_s = z_s/z_i$, with $z_s = h_s + \Delta h$, h_s being the source height and Δh being plume rise; either approach could be used with any of the σ_y parameterizations deemed appropriate, e.g., Eq. (3). Another alternative is Venkatram's (1980) touchdown model, which includes plume rise implicity. In the first draft, I had avoided making a clear recommendation, because this seemed to require extensive and time-consuming testing against data in order to be honest and helpful. After review, I decided to attempt clarification by comparing many of these parameterizations with a very accessible data base, the Dickerson (D) and Morgantown (M) power plant plume observations reported by Weil (1977) (these were also tabulated in part and used by Venkatram, 1980). Because of the limitations of these data, what follows must be considered somewhat speculative, and is new material, not a review of existing literature. However, I found this exercise necessary in order to discriminate among the alternative models reviewed. Somewhat unexpectedly, clear trends were seen during limited-mixing, low wind speed cases which appear to require new modeling approaches; simple ones are suggested, but these require further testing (my own time limit did not permit this).

Venkatram (1980) noted a surprisingly good comparison between these data and an extremely simple model $(\sigma_y/z_i) \propto X$ and $C_y = 1$, which represents uniform vertical mixing between $z = 0$ and $z = z_i$. This gave, for the centerline concentration, $\chi_c = 0.9Q/(w^* z_i X)$, with no dependence on wind speed. Using this result as a starting point, I calculated values of the ratio $w^* z_i X \chi_c/Q = X\underline{C}$, where $\underline{C} = U z_i^2 \chi_c/Q$, and discovered a strong relationship with another significant convectively scaled dimensionless parameter, $F^* = F_b/(U w^{*2} z_i)$, where F_b is the plume buoyancy flux. The largest values of $X\underline{C}$ are at $F^* < 0.007$, and there is a trend to smaller $X\underline{C}$ with larger F^*, beginning at about $F^* = 0.1$. For in between F^* values, there is no notable trend; $X\underline{C} \approx 0.9$ for D data points and ≈ 1.25 for M data points. Subsequent plots with less than linear growth assumptions for σ_y/z_i vs. X virtually eliminated the difference between D and M average values, without changing the overall relationship with F^*. [Values of X ranged roughly 3 times as large at Morgantown (M), probably because the plume was sampled by repeated traverses with a van traveling along roads and highways. The Morgantown plant is located on the shore of Potomac River tidewater, with water preventing the continuity of roads 10 to 25 km from the plant in most compass directions; x ranged up to 32 km, and the median distance was 18 km. The Dickerson plant is located in rolling terrain, with no large water bodies nearby.]

Because the smallest F^* cases are associated with smallest plume rise, compared to z_i, and also with smallest X, it is not surprising that $C_y > 1$ for most of these. Two possible effects of large F^* values, approximately 0.1 and greater, were recognized and discussed at the AMS/EPA Workshop on Updating Applied Diffusion Models in January 1984, although quantitative information was extremely sparse at the time. First, the plume can loft or bump against the top of the mixing layer with enough buoyancy to induce increased lateral spread, like that of hot smoke impinging upon a ceiling. Second, the residual buoyancy can resist downward mixing by convective eddies, at least until the plume thins sufficiently because of lateral spread. Of course, if the lofted plume is very buoyant at $z = z_i$, it can penetrate the capping inversion, but there is an intermediate range for which penetration is not significant. Recent photographic measurements of laboratory plumes by Willis and Hukari (1984) show crosswind-integrated plumes for $F^* = 0.08$ and 0.12 cases that rise coherently and loft just beneath $z = z_i$, with no concentration reaching the ground until $X \approx 1$; even at $X = 2.5$, most of the material is still lofted above $0.7 z_i$, and C_y is only about 0.5 at the surface. This behavior contrasts with the $F^* = 0.026$ case, which shows two almost-equal modes of C_y at $X \approx 1$, one just below z_i and one near the surface.

I tried more than a dozen plots of the D and M data to explore F^* effects, but must limit this discussion to the most significant plots, starting with σ_y. A plot of (σ_y/z_i) vs. X, similar to Fig. 1, definitely suggests enhancement of σ_y for the larger F^* cases, when these points are flagged. Figure 5 shows this plot without $F^* > 0.06$ cases, to establish a reference curve with almost no F^* effect. These points scatter over a factor of 3 range, approximately, and are fit rather well by Lamb's (1979) formulation, Eq. (2), times a factor of 1.5. The same could be said of a fit to Eq. (3) in the range $1 < X < 10$. A formulation similar to Eq. (3), which preserves the better established small-X asymptote is $\sigma_y/z_i = 0.6X/(1 + 0.6X)^{1/2}$. We should note that these are surface values of σ_y; the Morgantown points shown in Fig. 1, which better fit Eq. (3), are based on vertically integrated plumes, from a later experiment at the same plant. Thus, these plumes may broaden near the surface as they impinge on the ground.

The filled symbols in Fig. 5 are all the data points with $1.5 \leq U/w^* \leq 6$, the range of validity of convective scaling suggested by Deardorff and Willis (1975). These

are the runs used by Venkatram (1980). I added very low wind speed cases, $U/w^* < 1.5$, as open circles, to see how well or poorly moderate U/w^* relationships work for very low wind speeds; these cases represent very convective conditions, with $|z_i/L| > 100$; there are presently no alternatives to convective scaling for such conditions. The low U/w^* points tended to considerably increase the scatter in all data plots, until I applied a screening criterion based on the dimensionless sampling time $T_s = t_s U/z_i$ (t_s was taken to be $(N - 1)/N$ times the total length of time spent traversing the plume, where N is the number of traverses in a run; thus, it is the mean time from the first traverse to the last traverse across the center of the plume). Typically $T_s = 1.5$ is enough time for the passage of a single downdraft past a point. I found that all $T_s < 7$ points fell on the low side of all σ_y plots, especially the smallest T_s (≈ 2) points. These are probably inadequate sampling times. By removing all $T_s < 7$ runs, 5 of the 11 low U/w^* runs and 5 of the 48 moderate U/w^* runs were lost, but all plots improved. In Fig. 5, there are only 3 cases with $U/w^* < 1.5$, but they do fit in with the rest of the points.

Figure 6 explores the influence of F^* on σ_y by using Lamb's equation for $X > 1$ times 1.5 as a reference, $\sigma_y/z_i = 0.5X^{2/3}$ (in Fig. 5, this also fits the few $X < 1$ points adequately). This is especially convenient, because the $x^{2/3}$ plume rise law suggests a plume diameter enhancement due to entrainment that is proportional to $F_b^{1/3}U^{-1}x^{2/3} = z_i X^{2/3} F^{*1/3}$. Such a term appears in both Eqs. (7) and (8), from Weil (1979) and Venkatram (1980), respectively. Furthermore, the same $x^{2/3}$ law applies to the lateral spread of the turbulent, buoyant line thermal halted vertically by a horizontal plate, which resembles the situation of a bent-over, buoyant plume lofted against a capping inversion at $z = z_i$. According to a survey of laboratory measurements by Chen (1980), the plume half-width averages $2.8(F_b/U)^{1/3}(x/U)^{2/3}$ (I have taken the liberty of replacing line source strength with F_b/U, which is the buoyancy per unit length of bent-over plume, and time with x/U). In Fig. 6, the median of $(\sigma_y/z_i)X^{-2/3}$ is 0.5 for $F^* < 0.03$, and the median of each grouping of points for $F^* > 0.03$, excluding the small U/w^* cases, falls close to the curve $\sigma_y = 1.6 z_i X^{2/3} F^{*1/3} = 1.6 F_b^{1/3} U^{-1} x^{2/3}$; this curve represents purely buoyant growth, unaffected by CBL parameters except wind speed. While the coefficients in Eq. (7) (Weil, 1979) could be increased to fit the asymptotes in Fig. 7, at intermediate F^* values the vectorial addition would increase the predicted σ_y by about 40%, which would exceed all data points except for a few high outliers; the bulk of the data indicate a more abrupt change in slope with increasing F^*. Some of the high outliers may have been affected by wind

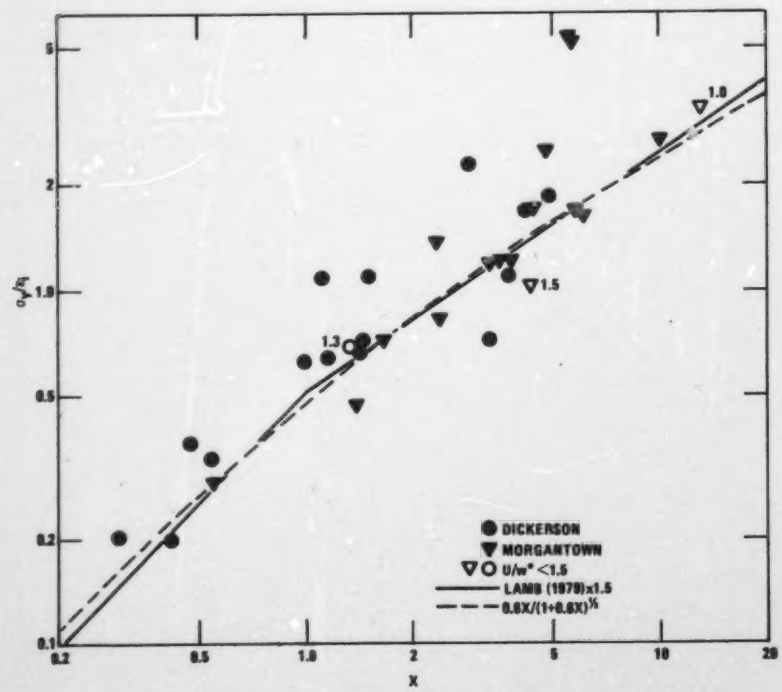

FIG. 5. Lateral dispersion, nondimensionalized by z_i, vs $X = (x/U)w^*/z_i$ for $F^* < 0.06$ cases, power plant data (Weil, 1977). $T_s < 7$ cases are excluded (small dimensionless sampling times; see text). Numbers indicate U/w^*, when this ratio < 1.5.

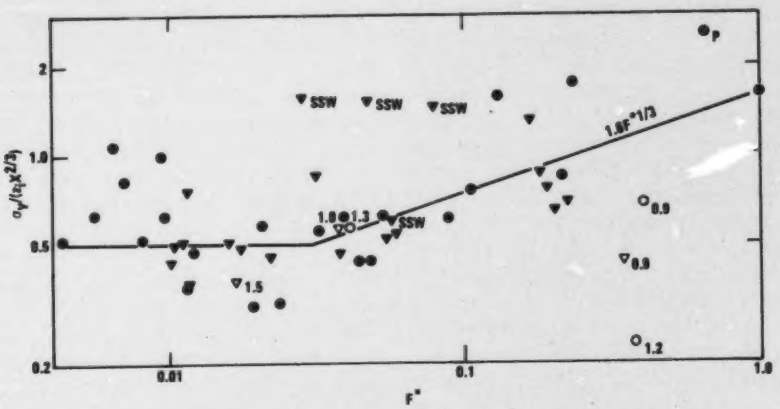

FIG. 6. Lateral dispersion, nondimensionalized by $z_i X^{2/3}$, vs $F^* = F_b/(Uw^{*2}z_i)$, power plant data (Weil, 1977). $T_s < 7$ cases are excluded. "SSW" indicates wind direction with overwater fetch immediately upwind of plant. "P" indicates a case for which partial penetration into capping layer is likely. Symbols and numbers same as in Fig. 5.

direction shifts; curiously, 3 of the 4 Morgantown runs with SSW winds, which were taken on four different days, are very high outliers; this is probably a site anomaly relating to the large overwater fetch. The point marked "P" is possibly a case in which the plume could partially penetrate the capping inversion; this was the lowest z_i case, with z_i only 70 m or so above the stack (z_i was measured with no better than ±25 m precision).

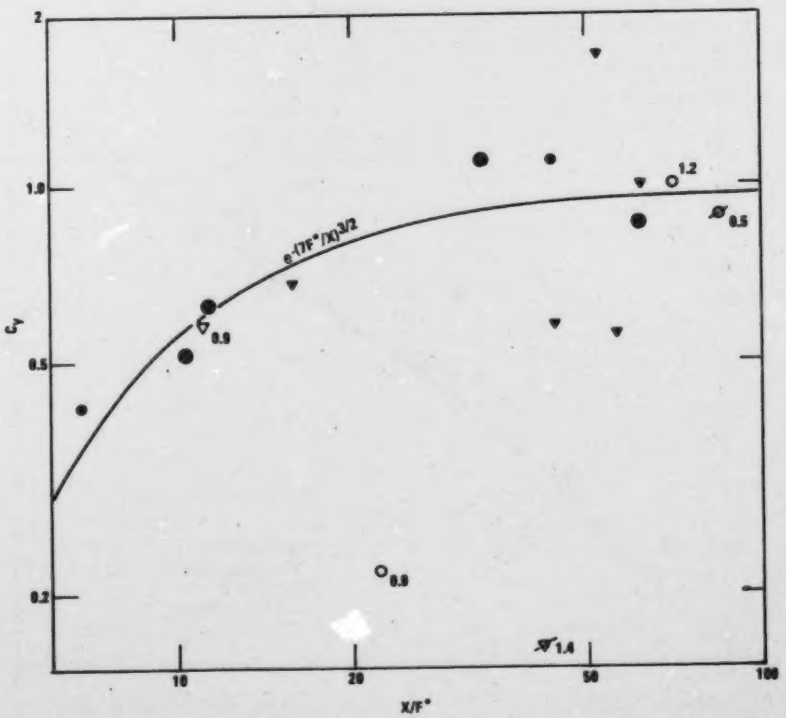

FIG. 7. Crosswind-integrated surface concentration, nondimensionalized as $C_y = z_i U \int \chi dy / Q$, vs $X/F^* = xw^{*3}/F_b$ for $F^* > 0.1$ cases, power plant data (Weil, 1977). $T_s < 7$ cases are slashed. Symbols and numbers same as in Fig. 5, except large symbols indicate $T_s > 40$ (large dimensionless sampling times).

A simple index of penetration ability is the excess temperature of a plume arriving at z_i with a cross sectional area $\pi(0.5\Delta h)^2$, which is $\Delta T = 4(T/g)(F_b/U)(z_i - h_s)^{-2}$ (Briggs, 1969). This excess temperature is 2.2°C for the "P" case, and only 0.4°C or less for all other points.

For the very low wind speed cases, $U/w^* < 1.5$, the few $F^* < 0.06$ data points fit in with the others, but the 3 points with $F^* \approx 0.4$ have large scatter and show no F^* enhancement of σ_y. According to the ⅔ law of plume rise, $\Delta h = 1.6F_b^{1/3}U^{-1}x^{2/3}$ (Briggs, 1984), the slope of a buoyant plume at $\Delta h = 0.8z_i$ is $d\Delta h/dx = 1.5F^{*1/2}w^*/U$. Thus, these 3 points are marginal cases of "bent-overness." We can draw no firm conclusions from these 3 cases, but recommend special attention to large F^*, small U/w^* situation, since these can give very large predicted ground concentrations, owing to the combination of small U and small z_i.

An $F^{*1/3}$ enhancement of plume width is not enough to account for the downward turn in χ_c in these data for $F^* > 0.1$. The dimensionless crosswind integrated concentration, C_y, which eliminates the σ_y effect, appears to trend downward also. Since $\int \chi dy$ was not reported, I had to estimate it using χ_c and σ_y with Eq. 14, which assumes a Gaussian lateral distribution; thus, $\int \chi dy = (2\pi)^{1/2}\chi_c\sigma_y$. I found no definite trend in $C_y = z_iU \int \chi dy/Q$ for $F^* < 0.1$ and $X > 1.4$, which is enough distance for roughly uniform vertical mixing of a passive plume in the CBL. However, the scatter is quite large, with about 25% of the points falling outside a ± factor of 2 limit. Curiously, there is much less scatter in $CX^{2/3}$, a form of C_y that uses an assumed, rather than a measured value of σ_y; if $\sigma_y/z_i \approx 0.5X^{2/3}$, then $C_y \approx 1.25CX^{2/3}$. With this assumption, the median values of C_y are 0.84 for D and 1.15 for M. All 24 moderate U/w^* points fall within a factor of 2 of $CX^{2/3} = 0.8$, and 80% fall inside a factor of 1.5 limit. The three $U/w^* < 1.5$ points show larger scatter, being both above and below $C_y = 1$ by factors of about 2.3. We can conclude that for $X > 1.4$ and $F^* < 0.1$, $C_y \approx 1$ for these data, with D data averaging slightly lower and M data slightly higher. We can also say that there is more scatter in $C\sigma_y/z_i$ than in $CX^{2/3}$, which implies that χ_c can be predicted with better accuracy than $\int \chi dy$. Fortunately, the main use of $\int \chi dy$ is for long-term averages, so this scatter in ~1-h ratios of observed to predicted C_y is not of much importance.

For $F^* > 0.1$ cases, we could derive an empirical C_y versus F^* relationship from these data, but there is only one data point beyond $F^* = 0.25$, at $F^* = 1.0$, free of complicating factors (large ΔT at $z = z_i$ or small U/w^*). This approach really would not be reasonable, because *eventually* any gaseous material trapped in the CBL will become uniformly vertically mixed, with $C_y = 1$. A number of simple theoretical approaches predict mix-down of lofted buoyant plumes at $X \propto F^*$, or $x \propto F_b/w^{*3}$. For instance, the speed of lateral spread, $\propto (F_b/x)^{1/3}$, reduces to the order of w^* at such a distance. Figure 7 shows C_y versus X/F^* for all $F^* > 0.1$ data. At $X/F^* > 30$, there is good support for $C_y \approx 1$. At smaller X/F^*, all points fall at $C_y < 0.7$. An empirical fit to most of these data points is given by

$$C_y = \exp[-(7F^*/X)^{3/2}]. \quad (23)$$

One of the 3 points with $U/w^* < 1.5$ and $T_s > 7$ is an outlier, with C_y a factor of 3.5 low, but the other 2 fall quite close to Eq. (23). This equation must be considered tentative, because of the small number of data points. For all $F^* > 0.1$ cases, $X > 2.5$ in these data, distances for which passive plume measurements indicate $C_y \approx 1$. The lack of data here at $X/F^* < 7$ probably reflects the desire of the observation team to make van traverses only at distances where the plume was in substantial contact with the ground. More support for the concept of delayed downward mixing at large F^* can be gleaned from the most recent laboratory tank results of Deardorff and Willis (1984). Dyed, buoyant plumes were released from a towed stack, and C_y was measured near the surface using the net absorption of a laser beam traversing the plume. Five experiments with $F^* = 0$ and 0.11 were performed and averaged. The $F^* = 0$ cases show the expected sharp peak in C_y versus x, roughly consistent with the prediction of Eq. (22) if $Z_s \approx ¼$ (h_s/z_i was 0.134, but some plume rise is evident in the photograph for this case). In contrast, the $F^* = 0.11$ cases show zero C_y at the surface until $X/F^* \approx 6$, then C_y increases rapidly to 0.3 at $X/F^* \approx 9$ and more slowly to 0.9 at $X/F^* \approx 30$. Although C_y rises more slowly with X at first, the laboratory results seem reasonably consistent with Eq. (23) and the power plant data shown in Fig. 7.

Incidentally, for large F^* compared to h_s/z_i and for large X, Venkatram's downdraft model of 1980 predicts $C_y = 0.5$ at $X/F^* = 8$, which is also supported by Fig. 7. This is a fortuitous result for $F^* > 0.2$ cases, because the top of the plume would reach z_i before this distance; the plume would be too large to be immersed in a single downdraft. However, a fortuitous model can be a useful tool, if it contains the fundamental parameters.

For $F^* > 0.1$, Eq. (23) can be combined with the σ_y estimate from Fig. 6 for large F^*,

$$\sigma_y/z_i = 1.6F^{*1/3}X^{2/3}. \quad (24)$$

to give a prediction of maximum centerline ground concentration, χ_{cmax}. Again, we use $\chi_c = \int \chi dy/[(2\pi)^{1/2}\sigma_y]$. Setting the derivative with respect to X equal to zero, we find a maximum at $X \approx 12F^*$, or $x \approx 12F_b/w^{*3}$ (for the D and M data, I would ascribe a factor of 2 uncertainty in the values of w^{*3}, so the approximation sign is highly advised). This gives the simple result that $C_{max} \approx 0.03F^{*-1}$, or

$$\chi_{cmax} \approx 0.03Qw^{*2}/(F_bz_i). \quad (25)$$

The absence of wind speed may seem strange, but this often occurs in models for convective conditions because of the widening of the plume as U gets small. Considering the measurement uncertainties, the small number of $F^* > 0.1$ runs, and the large stochastic vari-

ations in averages at small U, I would suggest a factor of 2 uncertainty in the constant in Eq. (25), until a larger body of data is examined. However, the laboratory tank results of Deardorff and Willis (1984) for $F^* = 0.11$ give good support to Eq. (25), with only ~15% larger peak occurring at $X/F^* \approx 9$; thereafter, the centerline concentration decreases extremely slowly, so that Eq. (25) is actually a good estimate from $X/F^* = 8$ to 36.

Buoyancy effects on σ_y and on C_y at $X > 1.4$ having been covered, buoyancy effects on C_y at smaller X need to be addressed. For $F^* > 0.1$ or so, Eq. (23) provides a simple solution, although it lacks testing at $X < 7F^*$, where it implies that $C_y < 0.4$. For smaller F^* and $X < 1.4$, it turns out that we can test a variety of C_y parameterizations by plotting data in the form $C_yZ_s = z_sU\int \chi dy/Q$ versus $X/Z_s = (w^*/z_s)x/U$. If we neglect the terms representing reflection from $z = z_i$, which do not contribute substantially to C_y until $X > 1.4$ to 2, anyway, most of the C_y models given in section 5 can be expressed in terms of C_yZ_s versus X/Z_s, which greatly simplifies intercomparison. The Venkatram (1980) model and Eq. (22) cannot, but they can be put approximately in this form, as will be shown in Fig. 8b. In order to do this for buoyant plumes, we must use a plume rise equation to get $z_s = h_s + \Delta h$. The literature contains a plethora of plume rise models, but there are only a few designed specifically for rise limited by convective turbulence. I chose the simple formula recommended in Briggs (1984),

$$\Delta h = 3(F_b/U)^{3/5}H^{*-2/5}, \quad \text{or} \quad \Delta h/z_i = 3F^{*3/5}. \quad (26)$$

This is thought to be slightly conservative (low), but appropriate data for directly testing any equation for Δh in convective conditions are extremely sparse. Equation 26 was recommended mostly on the basis of success in predicting observed maximum ground concentrations, using a Gaussian plume model. Note that for $F^* > 0.1$, Eq. (26) gives $\Delta h > 0.75z_i$ for the plume centerline, so the top of the plume would certainly be "bumping" against $z = z_i$ (therefore, do not use this equation for $F^* > 0.1$). This seems quite in line with the trends in C_y seen in the D and M data presented here.

By using $Z_s = h_s/z_i + 3F^{*3/5}$, all D and M data for $X < 2$ are plotted in Fig. 8a in C_yZ_s versus X/Z_s coordinates. The only exclusions are the "bumping" cases, $F^* > 0.1$, which all give the unacceptable result $Z_s > 1$; the five small sampling time cases, with $T_s = 4$ to 7, are kept in this plot but are flagged, since several appear to be outliers. There is only slight evidence of a peak in C_yZ_s near $X = 2Z_s$; if there is truly a peak, it is obscured by the scatter and the relatively small range of X/Z_s (again, we might suspect that the mobile van team did not care to sample at too small a distance, where the plume seldom hit the ground). Nonetheless, most points fall near the Gaussian plume model prediction, which peaks at $X/Z_s = 2$; the only assumption here, outside of the Gaussian one, is that $\sigma_z/z_i = 0.5X$, a slightly slower σ_z growth than assumed by Weil and Brower (1982), Eq. (12). This gives a better fit, and it is reasonable to expect that plume growth slows down a little as the ground is approached. The dashed line in Fig. 8a shows the effect of reflection

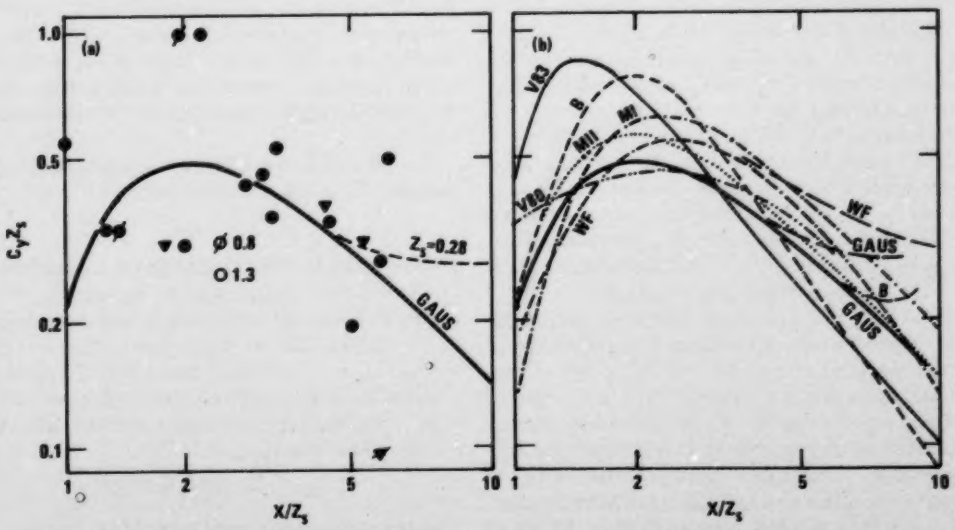

FIG. 8. (a) Crosswind-integrated surface concentrations, nondimensionalized as $C_yZ_s = z_sU\int \chi dy/Q$, vs $X/Z_s = (x/U)w^*/z_s$ for $X < 2$ cases, power plant data (Weil, 1977), $\Delta h/z_i = 3F^{*3/5}$ assumed in computing Z_s. $T_s < 7$ cases are slashed. Symbols and numbers as in Fig. 5. (b) Comparison of the predictions of the following models: Venkatram (1983), V83; Misra (1982), modifications I and II (in text), MI and MII; Equation 22, B; Venkatram (1980); V80; Weil and Furth (1981), WF; Gaussian, with $\sigma_z = 0.5(w^*/U)x$, GAUS.

from $z = z_i$ for a specific value of Z_s, 0.28; some 55% of the calculated Z_s values fall within 0.28 ± 0.04.

Figure 8b shows in identical coordinates the predictions of a half dozen other models besides the Gaussian one. Most are surprisingly similar, except that the Venkatram (1983) and the Briggs [Eq. (22)] parameterizations give a larger and narrower peak in C_yZ_s. The curve for the Venkatram (1980) model is not calculated, since this model does not start with an effective source height term, Z_s; it is a fit to the results of this model for D and M data for which Eq. (26) is used to determine Z_s for plotting on these coordinates, and fits all points within ±20%. Equation (22) is adapted to these coordinates by plotting the prediction for $Z_s = 0.28$; for other Z_s, the peak of C_yZ_s will increase by a factor $(Z_s/0.28)^{1/4}$, and the X/Z_s of the maximum will shift by $(0.28/Z_s)^{1/6}$, which is an insubstantial change for most D and M data points. Misra's formula for $Z_s = 0.24$, Eq. (19), is adapted to other Z_s by replacing $0.46/X$ with $1.9Z_s/X$ in the exponential (modification I). This, in effect, assumes no changes with height in the velocity statistics used in the model. Modification II of Misra's model is a readjustment of all the constants for a better fit to D and M data, with $C_yZ_s = 1.6(Z_s/X) \exp - (1.6Z_s/X - 0.2)^2$. The Weil and Furth (1981) curve is the first right-hand term of Eq. (18), and the Venkatram (1980) curve is the same for Eq. (20) [Eq. (21) is used for w^*p]. Reflection is shown as dashed lines only for $Z_s = 0.28$; these terms are very dependent on Z_s, since $C_yZ_s \approx Z_s$ at large X (the reflection calculation for the Venkatram (1983) model is omitted because it almost coincides with the "Gaussian" curve *without* reflection). Compared to most data plotted in Fig. 8a, both Eq. (22) and Venkatram (1983) curves are too peaky. Otherwise, considering the scatter and measurement uncertainties of these data, and considering the uncertainty in plume rise, all of the other models tested perform acceptably well. I would give a slight preference to Venkatram (1980), the Gaussian model, or Misra, modification II.

Except for Venkatram's (1980) model, these conclusions are dependent on the plume rise equation used to calculate Z_s, Eq. (26); similar conclusions would apply using other Δh models if they approximate Eq. (26), but if they predict a larger Δh, for instance, we would see larger peaks in the plotted C_yZ_s. For instance, if we used the plume rise recommended by Weil and Brower (1984), which is 1.43 times larger than that given by Eq. (26), the Z_s values used in Fig. 8a would be increased by about 27%, displacing all data points to the left and upward by a factor ≈1.27. In this case, Eq. (22) would be an acceptable fit to the data, and might provide the bridge that is needed between the passive and the strongly buoyant plume cases.

7. Discussion and interim recommendations

We have reviewed most published parameterizations for diffusion in the CBL to date. These include not only σ_y and σ_z, but also parameterizations for surface crosswind-integrated concentration. The latter are included to overcome deficiencies in Gaussian modeling, because in the CBL strongly non-Gaussian vertical diffusion has been observed for near-surface sources at $X > 0.5$ and for elevated sources in general. Since average concentrations are approximately Gaussian in the lateral direction, χ can be determined from $\int \chi dy$ and σ_y using Eq. (14). Some diffusion parameterizations include mechanical turbulence effects in the form of u^*, some include source height effects, and some include source buoyancy effects; the choice between alternatives is not always clear, but some attempt at sorting them out is made here. All recommendations for modeling of buoyant plumes were developed during the course of revising this paper, and must be held as especially tentative until data from a larger number of buoyant sources are examined, or reexamined. The present recommendations are based on my analysis of the mobile van measurements of surface SO_2 concentrations at the Dickerson and Morgantown power plants, reported by Weil (1977). In spite of the limitations of these data, they lend support to some of the recent ideas, and seem to require a new approach to other aspects of buoyant plume modeling.

All of the parameterizations involve the mixing depth, z_i, and the dimensionless distance $X = (x/U)w^*/z_i$. In comparing these parameterizations with schemes that use the variance of wind azimuth, σ_a, it is convenient to note that $\sigma_a \approx \sigma_v/U \approx 0.6w^*/U$ in the CBL, when $z_i > 15|L|$ or so and there are no sustained wind direction shifts during the sampling period of about 1 h. (Since individual convective downdrafts pass a point in a time $\sim 1.5z_i/U$, an adequate sampling period is 10 to $20(z_i/U)$; this period can actually range from about 10 min to many hours.) It is worthwhile to note that all convective diffusion parameterizations have a relatively weak dependence on heat flux and mixing depth at small x, usually through a term containing $w^* = (H^*z_i)^{1/3}$. At larger x, z_i inevitably becomes more important, especially for vertical diffusion; no realistic modeling effort can ignore the capping effect at $z = z_i$, or the effects of the dominant convective eddies, whose scale is limited by z_i. At the same time, the heat flux or H^* becomes even less influential, and can be considered noncritical. Suggestions for estimating these parameters using energy partitioning have been given in Briggs (1984), Sec. 8-5.5, and Holtslag and van Ulden (1983) (surface heat flux, Q, can be converted to H^* with sufficient accuracy using $H^* = 0.276(\text{cm}^2\,\text{s}^{-3})Q(1 + 0.13z_{MSL})$ where Q is in W m^{-2} and the elevation, z_{MSL}, is in km). It is also possible to estimate H^* in convective conditions from the measured potential temperature (θ) difference between two heights, as suggested by Dyer (1965):

$$H^* = 0.25(g/\theta)^{3/2}(\theta_1 - \theta_2)^{3/2}(z_1^{-1/3} - z_2^{-1/3})^{-3/2}. \quad (27)$$

For σ_y in convective conditions, at small X there is ample evidence supporting $\sigma_y \approx 0.6w^*x/U$. This is

consistent with $\sigma_y \approx \sigma_v t$ and many turbulence observations at various heights in the CBL that show $\sigma_v \approx 0.6w^*$; furthermore, it gives a good fit to $X < 0.4$ data in Fig. 1 and to $X < 1$ data in Fig. 5. Only the laboratory tank and numerical modeling results for elevated sources are systematically lower, by 20 to 40%. At larger x, there remains some discrepancy between these results and field measurements of σ_y. The Morgantown z-integrated plume σ_y in Fig. 1 average about 25% larger, and the Morgantown and Dickerson surface values of σ_y in Fig. 5 average about 50% larger than the laboratory and numerical results. This probably results from the effects of mesoscale eddies and possibly wind direction shear. Neither the convective tank nor the numerical model simulate eddies much larger than z_i, and the tank walls at $y = \pm 2z_i$ are a further constraint on lateral diffusion. Thus, Eq. 3 for σ_y, which is shown in Fig. 1, can be recommended as a *minimum* expected value, occurring in the absence of the larger scale effects.

However, it is not likely that the $\sigma_y \propto x^{1/2}$ asymptote, which is appropriate only when the plume is much wider than the largest mixing eddies, will hold true beyond travel time of 1 to 3 hours in the earth's atmosphere; mesoscale and synoptic-scale eddies and wind shifts are seldom absent for times much beyond the "spectral gap" at $t \sim 1$ h, and the diurnal cycle limits the domain of the convective steady-state approximation. The $X > 1$ approximation from Fig. 5, $\sigma_y = 0.5z_iX^{2/3}$, is probably more typical of real-world σ_y values measured near the surface. (This exceeds the Eq. (3) σ_y by 48% at $X = 2$, near the maximum X for the tank and numerical results.) Additional empirical support for $\sigma_y \propto x^{2/3}$ at large x is found in the approximation of Carras and Williams (1981) to observations of a very isolated plume in Australia; these aircraft measurements of plume width were made at $x = 15$ to 1000 km, with plume travel times of 1 to 40 hours. Their empirical fit to the observed plume widths has linear terms in t for growth during hours when the atmosphere is stable at plume height (~300 m), and $t^{2/3}$ growth for travel during convective hours, 1000–1800 LST. Assuming, as they do, that σ_y = plume width ÷ 4.28, their convective growth term for σ_y is $11.7t^{2/3}$. This corresponds to $0.5z_iX^{2/3}$ if $z_i = 1800$ m, as reported, and $H^* = 105$ cm^2 s^{-3}, which is a reasonable estimate for very dry terrain at 20° from the equator during the winter months. Considering all this, for typical applications in convective conditions I would recommend

$$\sigma_y = 0.6z_iX = 0.6w^*(x/U) \quad \text{at} \quad X < 0.6$$
$$= 0.5z_iX^{2/3} = 0.5H^{*2/9}z_i^{5/9}(x/U)^{2/3} \quad \text{at} \quad X > 0.6. \tag{28}$$

When $z_i/|L| < 30$, or $U > 5w^*$, mechanical turbulence can noticeably increase σ_v and σ_y, by 20% or more. Weil and Brower (1982) suggested a semiempirical formula including u^* [Eq. (4)], and Nieuwstadt and Van Duuren (1979) suggested a more elaborate and more theoretical formula along similar lines [Eq. (5)]. In consideration of the scatter in field observations of σ_y, I think that an adequate parameterization for now would be σ_y from Eq. (28) times a factor $(1 + (3u^*/w^*)^2)^{1/2}$. This approach resembles both Eqs. (4) and (5) at small X, and steers a middle course between simple empiricism and physical complexity at large X.

Equations (7) and (8), discussed at the end of section 3, give two different approaches for including the effect of buoyant rise on enhancement of σ_y. Neither of these formulas agrees well with the data analysis in section 6, which indicates considerably larger σ_y near the surface. Equation (28) gives a good fit to the power plant data in Fig. 5, which excludes large F^* cases. When $F^* = F_b/(Uw^{*2}z_i) > 0.03$, Fig. 6 shows that the data are approximated better by the $x^{2/3}$ law for buoyant plumes, specifically, $\sigma_y \approx 1.6F_b^{1/3}U^{-1}x^{2/3}$ [Eq. (24)]. The transition between Eq. (28) and Eq. (24) asymptotes is rather abrupt, so that adding them vectorially does not give a good fit. While many of the Fig. 6 observations were made at $x = 15$ to 20 km, enhancement of σ_y by buoyancy probably tapers off at larger x, particularly after the plumes become uniformly mixed in the CBL, at $X > 30F^*$. A form like $\sigma_y = 0.5X^{2/3}(1 + 35F^*e^{-aX/F^*})^{1/3}$, with a ~ 0.02, has the desired properties, but has not been tested.

For σ_z, there are also a number of parameterizations to choose from. Lamb's [Eq. (9)] are based on standard deviations of particle heights from source heights, as is the Deardorff and Willis (1975) parameterization for low-level sources [Eq. (10)]. The elevated source parameterization of Weil and Brower (1982), Eq. (12), is based on $\sigma_z \approx \sigma_w t$ and observed limits of σ_w/w^* or σ_w/u^*. On the basis of the small-X crossover between the convective terms of Eqs. (10) and (12) (both contain u^* terms also), I suggest Eq. (10) for low-level sources with $Z_s < 0.07$; however, the u^* term should be increased by a factor 1.6, for reasons discussed in section 4 (i.e., multiply b' by 1.6). Also, the authors' caution that Eq. (10) not be used beyond $X = 0.5$ should be heeded, since concentrations tend to lift off the surface beyond this point, unless a conservative approach is desired (keeping the plume axis at $z = z_s$). Equation (12) can be used for $Z_s > 0.07$, but a Gaussian model with a plume axis at constant height cannot account for the effect of observed plume axis descent in the CBL on increasing maximum surface concentrations, which has been repeatedly observed for passive plumes. This should be less of a problem when the u^* term dominates, at $z_i/|L| < 5$, when the boundary layer is weakly convective [in this case, Eq. (12) might be improved by replacing 1.26 in the u^* term with 1.6 times b', from Eq. (10)]. Buoyancy effects can greatly affect vertical diffusion, but direct effects on σ_z are probably significant only when a plume impacts on a nearby, elevated receptor. For strongly buoyant plumes in convective conditions, but with $F^* < 0.1$, the analysis in

section 6 indicates that the Gaussian model with $\sigma_z/z_i = 0.5X$ models surface concentrations reasonably well if it is used with a somewhat conservative plume rise formula, Eq. (26). The same conclusion should hold using Eq. (12) for σ_z, since it gives only slightly faster growth. However, according to Briggs (1984), a "neutral" plume rise formula, rather than Eq. (26), should be used if both $U > 2.8F_b^{1/6}$ and $U > 1.2h_s^{1/3}$ (mks units).

For improved handling of the non-Gaussian CBL vertical diffusion effects on surface concentrations, I recommend a $C_y = uz_i \int \chi_0 dy/Q$ parameterization. This is especially needed if $X > 0.5$ or the effective source height exceeds $0.2z_i$, say. For a passive source, the peak value of C_y is increased over that given by Gaussian models by a factor $\approx(1 + 2Z_s)$ (Briggs, 1985). Several recent models simulate this effect by assuming initial dispersion to be governed by a downwardly skewed vertical velocity probability distribution, $p(w)$, as has often been observed in the CBL. The models make various assumptions about "particle trajectories" beyond the small-x stage and about $p(w)$. An alternative for passive sources is a direct analytical fit to the convectively-scaled results of Willis and Deardorff tank experiments, Eq. (22); this permits easy application of the experimental results to any source height, as long as $Z_s > 0.04$. For smaller Z_s, the Gaussian plume model with Eq. (10) for σ_z, with b' increased by a factor of 1.6, should give good results (i.e., $C_y = (2/\pi)^{1/2}(z_i/\sigma_z) \times \exp\{-[2(\sigma_z/z_s)^2]^{-1}\}$.

For buoyant plumes with $Z_s = (h_s + \Delta h)/z_i > 0.04$, Eq. (22) gives too large a peak in C_y if Eq. (26) is used for Δh. However, if one uses the larger plume rise recommended by Weil and Brower (1984), which is a factor of 1.43 times Δh in Eq. (26), an acceptable fit to these data can be obtained with Eq. (22); this approach is attractive in that Eq. (22) performs well compared to passive plume data, so may provide a versatile method when used with the above plume rise. It should not be used when the calculated $Z_s > 0.8$, as occurs when F^* exceeds 0.05 or so, as this implies "bumping" of the top of the mixing layer and substantial changes in plume dynamics, such as the enhancement of σ_y already discussed. In such cases, it would be better to use the approach suggested below for $F^* > 0.1$ cases. The "smeared touchdown" model of Venkatram (1980) also performs well in comparison to Weil's (1977) data, but these were used to optimize some of the modeling assumptions; this model handles plume buoyancy implicitly, so does not require an additional assumption for plume rise. However, it underestimates peak C_y values for passive plumes by about a factor 2; thus, I would recommend it only for large buoyant sources, such as power plants.

When $F^* < 0.1$ and $X > 1.4$, it is hard to improve upon the simplest of modeling assumptions, uniform vertical mixing between $z = 0$ and $z_i (C_y = 1)$. However, about ¼ of the data points for Morgantown and Dickerson (Weil, 1977) fall a little outside a factor of 2 error bar. There is much less scatter in $CX^{2/3}$, which equals $0.8C_y$ if $\sigma_y = 0.5z_iX^{2/3}$ and there is a Gaussian lateral plume distribution. For 80% of the points, $CX^{2/3} = 0.8$ within a factor of 1.5.

The most radical modeling changes are indicated when $F^* = F_b/(Uw^{*2}z_i)$ is about 0.1 or larger. These are conditions of large source buoyancy, low wind speed, and restricted z_i, which are often "worst case" conditions for power plants. As indicated by recent tank experiments on buoyant plumes by Willis and Deardorff (1983), a buoyant plume impinges on the "lid" at $z = z_i$ before surface impact occurs when $F^* > 0.1$. The residual buoyancy causes both enhanced σ_y, due to buoyancy-induced spread under the lid, and a delay in downward mixing; both of these efforts tend to reduce surface concentrations. We have already discussed F^* effects on σ_y. A further effect seen in the data analysis in section 6 is that plume impact at the ground is delayed in proportion to F_b/w^{*3}, or $X \propto F^*$. The data shown in Fig. 7 are fit by $C_y = \exp[-(7F^*/X)^{3/2}]$, Eq. (23). Combining Eqs. (23) and (24) results in a maximum surface concentration that is independent of wind speed, Eq. (25). When $F^* \sim 1$ or larger, consideration must also be given to the possibility that part or all of the plume penetrates out of the mixing layer; this depends on the strength of the capping inversion and overlying stratification; see Briggs (1984) or Weil and Brower (1984).

The scant number of data points for very low wind speeds, with $0.5 \leqslant (U/w^*) < 1.5$, acceptably fit most of the above conclusions, with a few points having much lower C_y. The main exception is that the three $F^* > 0.1$ points do not support F^* enhancement of σ_y; for these three cases, the calculated plume slope at $z = z_i$ is greater than 1, so the plumes do not arrive at $z = z_i$ fully bent over. It may be necessary to develop new models or model corrections for small U/w^*, large F^* cases.

REFERENCES

Agterberg, R., F. T. M. Nieuwstadt, H. van Duuren, A. J. Hasselton and G. D. Krijt, 1983: Dispersion experiments with sulphur hexafluoride from the 213 m high meteorological mast at Cabauw in the Netherlands. Royal Netherlands Meteorological Institute, De Bilt, 129 pp.

Barad, M. L. (ed.), 1958: Project Prairie Grass; a field program in diffusion. Geophys. Res. Paper No. 59, Vols. I and II, AFCRF-TR-58-235, Air Force Cambridge Research Center, Bedford, MA.

Briggs, G. A., 1969: *Plume Rise*. U.S.A.E.C. Critical Review Series TID-25075, NTIS, 81 pp.

——, 1982; Similarity forms for ground-surface surface-layer diffusion. *Bound.-Layer Meteor.*, **23**, 489–502.

——, 1984: Plume rise and buoyancy effects. Chapter 8 in *Atmospheric Science and Power Production*, D. Randerson, Ed., U.S. Dept. of Energy DOE/TIC-27601, p. 351. [Available from NTIS as DE84005177.]

——, 1985: Diffusion modeling with convective scaling and effects of surface inhomogeneities. *Proc. AMS Specialty Conference on Air Quality Modeling of the Urban Boundary Layer*, Baltimore, Amer. Meteor. Soc. (in press).

——, and K. R. McDonald, 1978: Prairie Grass revisited: optimum

indicators of vertical spread. *Proc. Ninth Int. Tech. Meeting on Air Pollution Modeling and its Application,* No. 103, NATO, 209–220. [Available as contribution 78/8, Atmospheric Turbulence and Diffusion Lab., Oak Ridge, TN 37830.]

Carras, J. N., and D. J. Williams, 1981: The long-range dispersion of a plume from an isolated point source. *Atmos. Environ.*, **15,** 2205–2217.

Chen, J. C., 1980: Studies on gravitational spreading currents. Rep. No. KH-R-40, W. M. Keck Laboratory of Hydraulics and Water Resources, CIT, Pasadena, CA, 436 pp.

Deardorff, J. W., 1970a: Preliminary results from numerical integrations of the unstable boundary layer. *J. Atmos. Sci.*, **27,** 1209–1211.

——, 1970b: Convective velocity and temperature scales for the unstable boundary layer for Rayleigh convection. *J. Atmos. Sci.*, **27,** 1211–1213.

——, 1972: Numerical investigation of neutral and unstable planetary boundary layer. *J. Atmos. Sci.*, **29,** 91–115.

——, and G. E. Willis, 1974: Computer and laboratory modeling of the vertical diffusion of nonbuoyant particles in the mixed layer. *Advances in Geophysics,* Vol. 18B, H. E. Landsberg and J. Van Mieghem, Eds., Academic Press, 187–200.

——, and ——, 1975: A parameterization of diffusion into the mixed layer. *J. Appl. Meteor.*, **14,** 1451–1458.

——, and ——, 1984: Groundlevel concentration fluctuations from a buoyant and a non-buoyant source within a laboratory convectively mixed layer. *Atmos. Environ.*, **18,** 1297–1309.

Draxler, R. R., 1976: Determination of atmospheric diffusion parameters. *Atmos. Environ.*, **10,** 99–105.

Dyer, A. J., 1965: The flux-gradient relation for turbulent heat transfer in the lower atmosphere. *Quart. J. Roy. Meteor. Soc.*, **91,** 151–157.

Gifford, F. A., 1961: Use of routine meteorological observations for estimating atmospheric dispersion. *Nuclear Safety,* **2(4),** 47–51.

——, 1975: Atmospheric dispersion models for environmental pollution applications. *Lectures on Air Pollution and Environmental Impact Analyses,* Amer. Meteor. Soc., Boston, 35–58.

Gryning, S-E., 1981: Elevated source SF_6 tracer dispersion experiments in the Copenhagen area. Riso-R-446, Riso National Lab., DK-4000, Roskilde, Denmark.

Holtslag, A. A. M., and A. P. van Ulden, 1983: A simple scheme for daytime estimates of the surface fluxes from routine weather data. *J. Climate Appl. Meteor.*, **22,** 517–529.

Kaimal, J. C., J. C. Wyngaard, D. A. Haugen, O. R. Cote, Y. Izumi, S. J. Caughey and C. J. Readings, 1976: Turbulence structure in the convective boundary layer. *J. Atmos. Sci.*, **33,** 2152–2169.

Lamb, R. G., 1978: A numerical simulation of dispersion from an elevated point source in the convective boundary layer. *Atmos. Environ.*, **12,** 1297–1304.

——, 1979: The effect of release height on material dispersion in the convective planetary boundary layer. *Preprints Fourth Symp. on Turbulence, Diffusion, and Air Pollution,* Reno, Amer. Meteor. Soc.

——, 1981: Diffusion in the convective boundary layer. *Proc. A Short Course on Atmospheric Turbulence and Air Pollution Modeling,* F. T. M. Nieuwstadt and H. van Dop, Eds., Reidel, 159–230.

Lenschow, D. H., 1970: Airplane measurements of planetary boundary layer structure. *J. Appl. Meteor.*, **9,** 874–884.

——, and P. L. Stevens, 1980: The role of thermals in the convective boundary layer. *Bound.-Layer Meteor.*, **19,** 509–532.

Misra, P. K., 1982: Dispersion of non-buoyant particles inside a convective boundary layer. *Atmos. Environ.*, **16,** 239–243.

Moninger, W. R., W. L. Eberhard, G. A. Briggs, R. A. Kropfli and J. C. Kaimal, 1983: Simultaneous radar and lidar observations of plumes from continuous point sources. *Preprints, 21st Radar Meteorology Conference,* Edmonton, Amer. Meteor. Soc., 246–250.

Nieuwstadt, F. T. M., 1980: Application of mixed-layer similarity to the observed dispersion from a ground-level source. *J. Appl. Meteor.*, **19,** 157–162.

——, and H. van Duuren, 1979: Dispersion experiments with SF_6 from the 213 m high meteorological mast at Cabauw in the Netherlands. Preprint, *Fourth Symp. on Turbulence, Diffusion, and Air Pollution,* Reno, Amer. Meteor. Soc., 34–40.

Panofsky, H. A., 1973: Tower micrometeorology. Chap. 4 of *Workshop on Micrometeorology,* D. A. Haugen, Ed., Amer. Meteor. Soc., Boston, p. 166.

——, H. Tennekes, D. H. Lenschow and J. C. Wyngaard, 1977: The characteristics of turbulence velocity components in the surface layer under convective conditions. *Bound.-Layer Meteor.*, **11,** 355–361.

Pasquill, F., 1961: The estimation of the dispersion of windborne material. *Meteor. Mag.*, **90,** 33–49.

——, 1976: Atmospheric dispersion parameters in Gaussian plume modeling. Part II: possible requirements for change in the Turner workbook values. U.S. Environmental Protection Agency, EPA-600/4-76-0306.

Singer, I. A., and M. E. Smith, 1966: Atmospheric dispersion at Brookhaven National Laboratory. *Int. J. Air Water Pollut.*, **10,** 125–135.

Tennekes, H., 1973: Similarity laws and scale relations in planetary boundary layers. Chap. 5 in *Workshop on Micrometeorology,* D. A. Haugen, Ed., Amer. Meteor. Soc., Boston, 177–216.

Venkatram, A., 1980: Dispersion from an elevated source in a convective boundary layer. *Atmos. Environ.*, **14,** 1–10.

——, 1983: On dispersion in the convective boundary layer. *Atmos. Environ.*, **17,** 529–533.

——, and R. Vet, 1981: Modeling of dispersion from tall stacks. *Atmos. Environ.*, **15,** 1531–1538.

Weil, J. C., 1977: Evaluation of the Gaussian plume model at Maryland power plants. Ref. No. PPSP-MP-16, Maryland Power Plant Siting Program, Martin Marietta Corp., Baltimore.

——, 1979: Assessment of plume rise and dispersion models using lidar data. Ref. No. PPSP-MP-24, Maryland Power Plant Siting Program, Martin Marietta Corp., Baltimore.

——, and W. F. Furth, 1981: A simplified numerical model of dispersion from elevated sources in the convective boundary layer. Extended abstract, *Fifth Symp. on Turbulence, Diffusion, and Air Pollution,* Atlanta, Amer. Meteor. Soc., 76–77.

——, and R. P. Brower, 1982: The Maryland PPSP dispersion model for tall stacks, Ref. No. PPSP-MP-36, Maryland Power Plant Siting Program, Martin Marietta Corp., Baltimore.

——, and ——, 1984: An updated Gaussian plume model for tall stacks. *J. Air Pollut. Control Assoc.*, **34,** 818–827.

Willis, G. E., and J. W. Deardorff, 1976a: A laboratory model of diffusion into the convective planetary boundary layer. *Quart. J. Roy. Meteor. Soc.*, **102,** 427–445.

——, and ——, 1976b: Visual observations of horizontal planforms of penetrative convection. Preprint, *Third Symp. on Atmospheric Turbulence, Diffusion and Air Quality,* Raleigh, NC, Amer. Meteor. Soc., 9–12.

——, and ——, 1978: A laboratory study of dispersion from an elevated source in a convective mixed layer. *Atmos. Environ.*, **12,** 1305–1313.

——, and ——, 1981: A laboratory study of dispersion from a source in the middle of the convectively mixed layer. *Atmos. Environ.*, **15,** 109–117.

——, and N. Hukari, 1984: Laboratory modeling of buoyant stack emissions in the convective boundary layer. Conference volume, *Fourth Joint Conf. on Applications of Air Pollution Meteorology,* Portland, Amer. Meteor. Soc., 24–26.

Wyngaard, J. C., O. R. Cote and Y. Izumi, 1971: Local free convection, similarity, and the budgets of shear stress and heat flux. *J. Atmos. Sci.*, **28,** 1171–1182.

Yaglom, A. M., 1972: Turbulent diffusion in the surface layer of the atmosphere. *Izv. Atmos. Oceanic Phys.*, **8,** 333–340.